Nonsulfide and sulfide-rich zinc mineralizations in the Vazante, Ambrósia and Fagundes deposits, Minas Gerais, Brazil: Mass...

Article *in* Gondwana Research · April 2007

DOI: 10.1016/j.gr.2006.04.017

CITATIONS
15

READS
189

4 authors, including:

Lena Virgínia Soares Monteiro
University of São Paulo
50 PUBLICATIONS **472** CITATIONS
SEE PROFILE

Jorge Silva Bettencourt
University of São Paulo
83 PUBLICATIONS **1,350** CITATIONS
SEE PROFILE

Caetano Juliani
University of São Paulo
73 PUBLICATIONS **485** CITATIONS
SEE PROFILE

Available online at www.sciencedirect.com
ScienceDirect
Gondwana Research 11 (2007) 362–381
www.elsevier.com/locate/gr

Nonsulfide and sulfide-rich zinc mineralizations in the Vazante, Ambrósia and Fagundes deposits, Minas Gerais, Brazil: Mass balance and stable isotope characteristics of the hydrothermal alterations

Lena Virgínia Soares Monteiro [a,*], Jorge Silva Bettencourt [b], Caetano Juliani [b], Tolentino Flávio de Oliveira [c]

[a] *Instituto de Geociências, Universidade Estadual de Campinas, R. João Pandiá Calógeras, 51, CEP 13083-970, Campinas, SP, Brazil*
[b] *Instituto de Geociências, Universidade de São Paulo, Rua do Lago, 562, CEP 05508-080, São Paulo, SP, Brazil*
[c] *Votorantim Metais, Caixa Postal 3, CEP 38780-000, Vazante, MG, Brazil*

Received 31 January 2004; accepted 24 April 2006
Available online 9 August 2006

Abstract

The Vazante Group hosts the Vazante nonsulfide zinc deposit, which comprises high-grade zinc silicate ore ($ZnSiO_4$), and late-diagenetic to epigenetic carbonate-hosted sulfide-rich zinc deposits (e.g. Morro Agudo, Fagundes, and Ambrósia). In the sulfide-rich deposits, hydrothermal alteration involving silicification and dolomitization was related with ground preparation of favorable zones for fluid migration (e.g. Fagundes) or with direct interaction with the metalliferous fluid (e.g. Ambrósia). At Vazante, hydrothermal alteration resulted in silicification and dolomite, siderite, jasper, hematite, and chlorite formation. These processes were accompanied by strong relative gains of SiO_2, $Fe_2O_{3(T)}$, Rb, Sb, V, U, and La, which are typically associated with the nonsulfide zinc mineralization. All sulfide-rich zinc ores in the district display a similar geochemical signature suggesting a common metal source from the underlying sedimentary sequences.

Oxygen and carbon isotope compositions of hydrothermally altered rocks reveal a remarkable alteration halo at the Vazante deposit, which is not a notable feature in the sulfide-rich deposits. This pattern could be attributed to fluid mixing processes involving the metalliferous fluid and channelized meteoric water, which may control the precipitation of the Vazante nonsulfide ore. Sulfide deposition resulted from fluid–rock interaction processes and mixing between the ascending metalliferous fluids and sulfur-rich tectonic brines derived from reduced shale units.

Keywords: Nonsulfide; Carbonate chemistry; Willemite; Hydrothermal alteration; Stable isotopes

1. Introduction

The Neoproterozoic Vazante Group located in the northwest part of Minas Gerais State, Brazil, hosts nonsulfide (Vazante) and sulfide-dominated zinc deposits (Morro Agudo, Ambrósia, and Fagundes). The occurrence of both types of deposits in the same district is uncommon, but it was also reported in Namibia (Neoproterozoic Otavi Group, Chetty and Frimmel, 2000) and in Zambia (Katangan Supergroup, Kamona et al., 1999).

The Vazante deposit is one of the major known nonsulfide zinc deposit in the world (Hitzman et al., 2003), and includes ore types characterized by predominance of hemimorphite or willemite. The hemimorphite-rich ore is associated with karst-related collapse breccias developed in pelitic–dolomitic units of the Neoproterozoic Vazante Group (Dardenne, 2000) and controlled by NE-oriented brittle faults and fractures. The willemitic ore (18.8 Mt at 23.7% Zn; T.F. Oliveira, 2006; personal communication) is structurally controlled and occurs imbricated with small sulfide-rich ore, hydrothermally altered dolostones, slates, and metabasites.

These ore types have been regarded as being of supergene origin since the 1960s. However, whereas this hypothesis is considered consensual for the hemimorphite-rich ore (Amaral, 1968; Rigobello et al., 1988), different genetic models have

* Corresponding author.
E-mail addresses: lena@ige.unicamp.br (L.V.S. Monteiro), jsbetten@usp.br (J.S. Bettencourt), cjuliani@usp.br (C. Juliani), flavio@vz.cmm.com.br (T.F. de Oliveira).

1342-937X/$ - see front matter © 2006 International Association for Gondwana Research. Published by Elsevier B.V. All rights reserved.
doi:10.1016/j.gr.2006.04.017

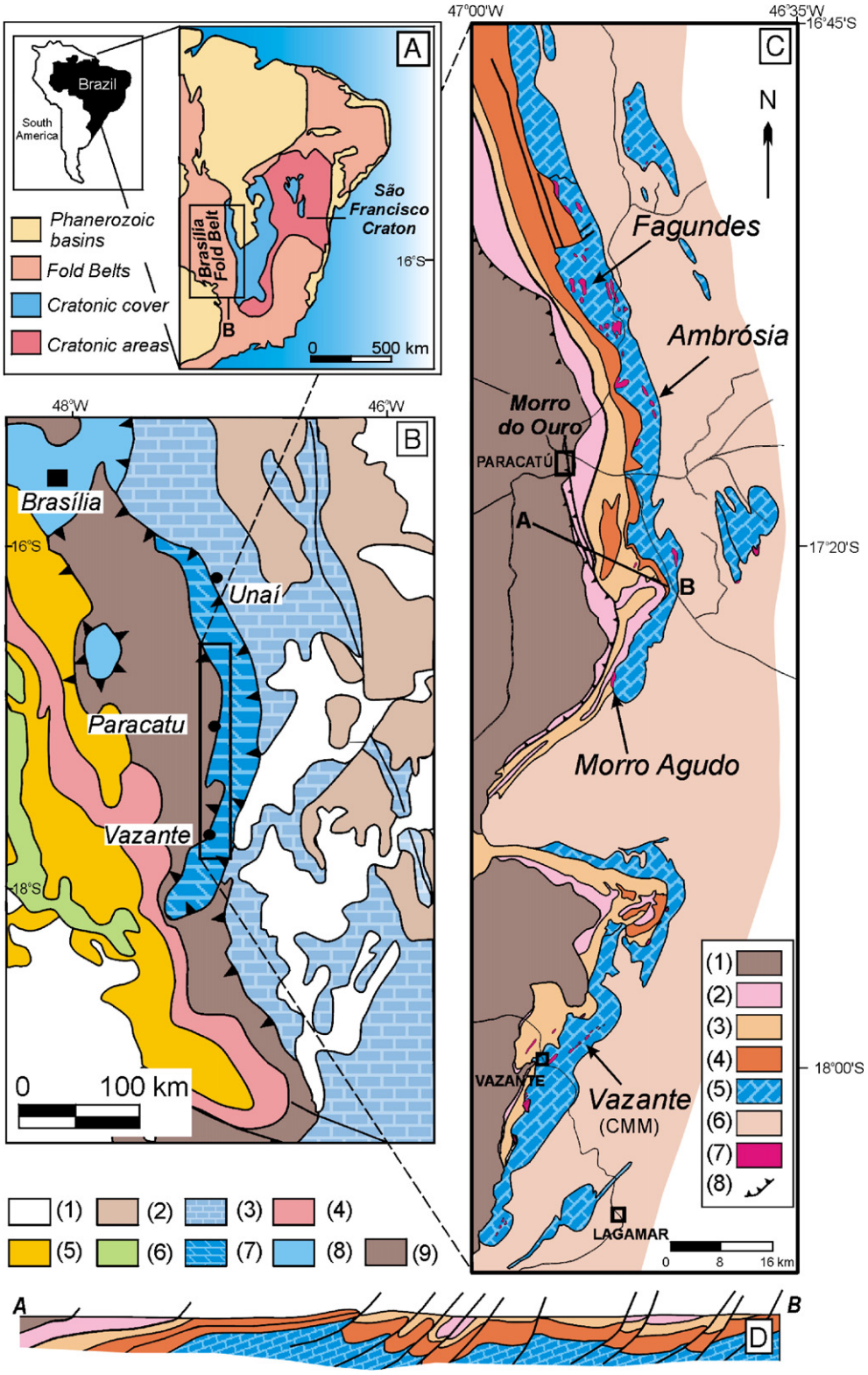

Fig. 1. (A) Location map of the Brasília Fold Belt and the São Francisco Craton (Dardenne, 2000); (B) Geological map of the southern segment of the Brasília Fold Belt (Dardenne, 2000): (1) Phanerozoic basins; (2) Bambuí Group, Três Marias Formation; (3) Bambuí Group, Paraopeba Subgroup; (6) Ibiá Formation; (7) Araxá Group; (8) Felsic and mafic granulites and orthogneisses; (9) Vazante Group; (10) Paranoá Group; (11) Canastra Group; (C) Geological map of the Vazante Group and location of the Vazante, Ambrósia and Fagundes deposits (Votorantim Metais). 1 and 2 = Canastra Group, (1) Paracatu Formation (carbonaceous phyllite with quartzite layers, (2) Serra do Landim Formation (green carbonate phyllite); 3 to 6 = Vazante Group, (3) Serra da Lapa Member, Lapa Formation (gray slate, quartzite and dolostone lenses), (4) Serra do Velosinho Member, Lapa Formation (black carbonaceous slate and shale), (5) Morro do Calcário and Serra do Poço Verde formations (stromatolitic bioherm, breccia facies, cyanobacteria-laminated dolostone; gray to pinkish dolostone with stromatolitic mats, gray to green slate), (6) Serra do Garrote Formation (black carbonaceous shale and gray slate); (7) Pb anomalies; (D) Cross-section of the Vazante Group (Oliveira, 1998). (For interpretation of the references to colour in this figure legend, the reader is referred to the web version of this article.)

been proposed for the willemitic ore. The occurrence, at surface, of willemite involving remains of sulfides strongly replaced by chalcocite, covellite, cerussite, and malachite with typical crustiform textures, was considered as evidence of the willemite secondary origin (Amaral, 1968). Petrographic studies indicate, however, that sphalerite replacement by willemite was previous to supergene mineral formation and controlled by the development of the Vazante Shear Zone (Pinho, 1990; Monteiro, 1997). Oxygen stable isotope geothermometers indicate relatively high temperatures (254 to 294 °C) for the willemitic ore (willemite–quartz and hematite–quartz pairs; Monteiro, 1997; Monteiro et al., 1999). Fluid inclusion studies in willemite (Dardenne and Freitas-Silva, 1999) also indicate homogenization temperature conditions (up to 180 °C) compatible with an epigenetic-hydrothermal origin for this ore type from mineralizing fluids at high fO_2/fS_2 (Monteiro, 1997; Monteiro et al., 1999; Hitzman et al., 2003). These conditions are consistent with those experimentally predicted by Brugger et al. (2003), leading to the formation of willemite instead of sphalerite, especially at temperatures higher than 150 °C.

Other deposits hosted by the Vazante Group include the Irish-type Morro Agudo zinc–lead deposit (Hitzman, 1997; Misi et al., 1999; Cunha et al., 2000; Misi et al., 2005) and several carbonate-hosted zinc deposits, including the late-diagenetic to epigenetic Fagundes and the epigenetic-hydrothermal Ambrósia zinc–lead deposits (Monteiro et al., 2000; Monteiro, 2002, 2006).

Despite the differences in mineralogy, alteration styles, ore controls and textures, the zinc deposits associated with the Vazante Group share some attributes, such as the dolomitic composition of the host rocks and the important role of high-temperature (>250 °C), moderate salinity, metalliferous fluids (Monteiro et al., 1999; Misi et al., 2005; Monteiro et al., 2006).

This paper aims to document a mass balance calculation of hydrothermal alteration and mineralization processes, together with elemental and isotopic compositions of the host dolostones and hydrothermal carbonates, and to characterize the extent of the geochemical processes associated with the genesis of non-sulfide and sulfide-rich zinc deposits of the Vazante Group. The study presents new data on the Vazante, Fagundes, and Ambrósia deposits, and permits a comparison with published data on the Morro Agudo deposit.

2. Geological setting

2.1. The Brasília Fold Belt

The Vazante Group (Dardenne, 2000), which hosts the zinc–lead deposits in the Vazante–Paracatu belt, lies on the western border of the São Francisco Craton and represents one metasedimentary unit of the southern segment of the Brasília Fold Belt (Almeida, 1967).

The Brasília Fold Belt, in central Brazil, extends for more than 1000 km over a width of 300 km along the western edge of the São Francisco Craton (Fig. 1A and B). The main stages of the tectonic evolution of this fold belt have been discussed in detail by Dardenne (2000) and Pimentel et al. (2001), and encompass two collisional events, one related to a magmatic arc–continent collision (ca. 0.79 Ga) and the other associated with a continent–continent collision (0.63–0.61 Ga). The latter represents the main metamorphic-deformational event within the Brasília Belt and is interpreted as indicative of the final closure of the ocean basin following the collision between the Amazon and the São Francisco–Congo continents (Pimentel et al., 2001).

The Brasília Belt includes in its eastern part a thick pile of sediments deposited along the western margin of the São Francisco–Congo Craton. Several lithostratigraphic units are identified (Araí, Paranoá, Serra da Mesa, Araxá, Ibiá, Vazante, Canastra, and Bambuí groups) and have been interpreted as part of a Meso- to Neoproterozoic passive margin of the São Francisco continent, with shallow water platformal sediments in the east, and deeper-water turbiditic sediments in the west (Dardenne, 1979; Pimentel et al., 2001).

These sedimentary rock units were progressively deformed and metamorphosed towards the west, ranging from undeformed and unmetamorphosed rocks in the cratonic area to amphibolite and granulite facies rocks in the west (Dardenne, 2000). In the southern segment of the Brasília Belt, the Araxá, Canastra, Ibiá, and Vazante groups have been involved in a complex imbricated system of nappes and thrusts, which obstruct the recognition of stratigraphic relationships between these rock units and, in some cases, even their internal stratigraphic organization.

2.2. The Vazante Group

The Vazante Group (Dardenne, 2000) extends up to 250 km along a N–S trend in the southern segment of the Brasília Fold Belt (Fig. 1B and C). It corresponds to a thick marine pelitic–dolomitic sequence affected by low greenschist facies metamorphism (Fig. 1D; Dardenne, 2000).

The Vazante Group is divided, from base to top, into seven formations, as illustrated in Fig. 2.

The Serra do Poço Verde and the Morro do Calcário formations correspond to the dominantly dolomitic units that host the Zn–(Pb) deposits. The Serra do Poço Verde Formation is divided into four members from base to top: the Lower Morro do Pinheiro Member is composed of dolostone with cyanobacteria mats, oncolitic dolarenite, intraformational breccias and lenses of dolostone with columnar stromatolites (500 m thick); the Upper Morro do Pinheiro Member comprises dark gray dolostone with cyanobacteria mats, bird's-eye features, marls, and pyrite-bearing carbonaceous shale (300–500 m thick); the Lower Pamplona Member, which hosts the Vazante mineralizations, is made of gray to pink micritic cyanobacteria-laminated dolostone, gray to green slates, and sericite phyllite (100–200 m thick); the Medium Pamplona Member comprises gray to pink dolostone, dolarenite, lamellar breccia, dolostone with columnar stromatolites, and shale lenses (400 m thick). The Morro do Calcário Formation corresponds to the Upper Pamplona Member of Rigobello et al. (1988), and is composed of stromatolitic bioherm and biostrome facies, breccias, oolitic and oncolitic dolarenite and dolorudite.

The dolomitic sequence is overlain by the Lapa Formation, with black carbonaceous slate and phyllite (Serra do Velosinho

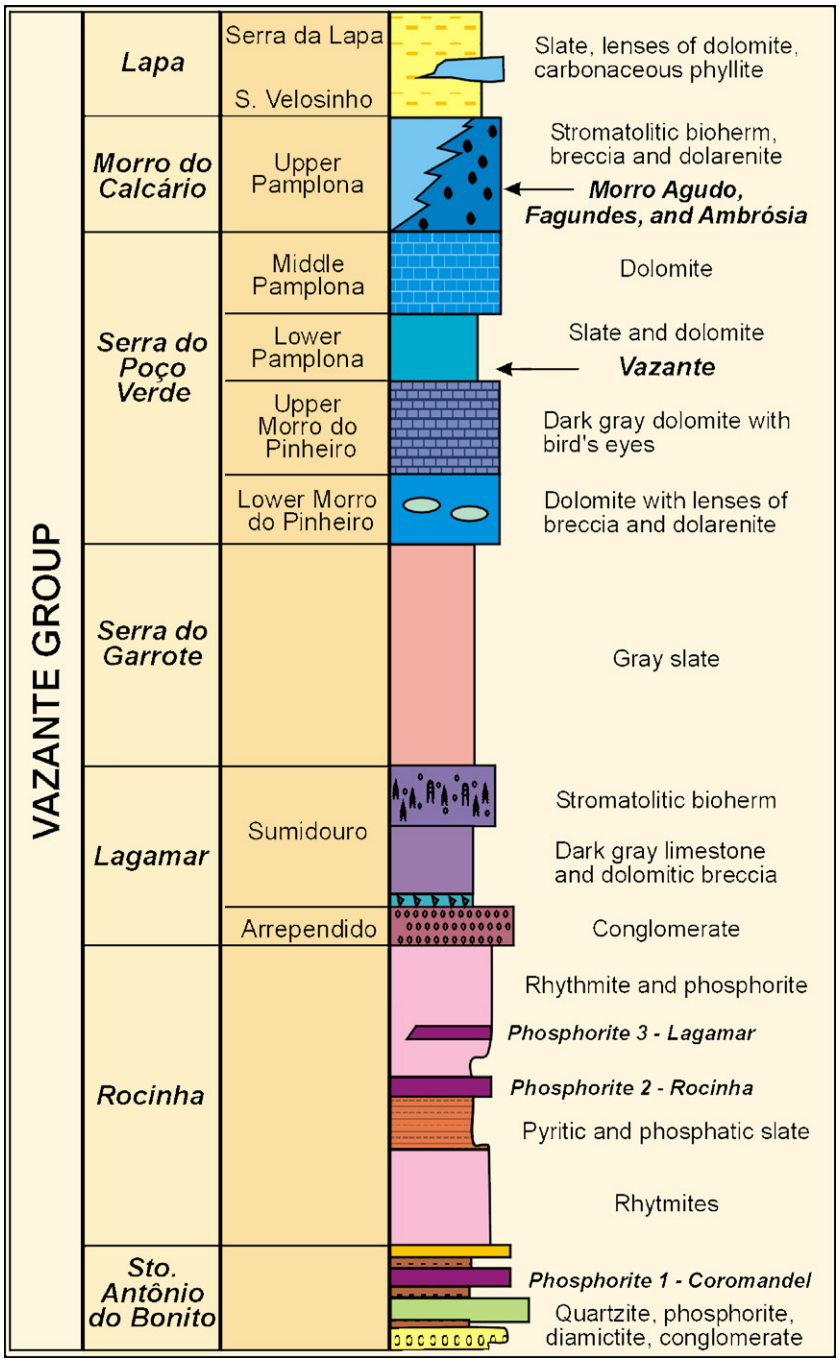

Fig. 2. Lithostratigraphic column of the Vazante Group (Dardenne, 2000).

Member), and by phyllite, carbonate-bearing metasiltstone, dolostone and quartzite lenses of the Serra da Lapa Member (Madalosso and Valle, 1978). Chlorite-rich calc-phyllite, carbonaceous phyllite, and quartzite of the Canastra Group (1.2–0.9 Ga; Pimentel et al., 2001) overthrust the rocks of the Vazante Group.

The geotectonic context of the Vazante Group is still disputable. Correlations have been proposed between the Vazante Group and the 1.2–0.9 Ga Paranoá Group or the 0.9–0.6 Ga Bambuí Group.

The Paranoá Group comprises basal paraconglomerate overlain by rhythmites with mudcracks and evaporite layers, typical of a tidal to supratidal environment, marine rhythmites, and quartzites, deposited in a platformal environment dominated by tidal currents, and deeper water pelites alternate with tidal rhythmites and quartzites, storm rhythmites, limestones, and stromatolitic dolomites (Dardenne, 2000). Correlation of the Vazante Group with this unit was based on the similarity of the stromatolites present in both groups (*Conophyton Cylindricus Maslov*, Moeri, 1972; *Conophyton metula Kirichenko*, Cloud and Dardenne, 1973).

The Bambuí Group, which occupies all of the eastern side of the Brasília Fold Belt and covers large areas of the São Francisco Craton, comprises basal conglomerate and diamictite

(Jequitaí Formation) of glacial origin and a platformal sequence represented by three regressive megacycles characterized by deep marine sequences at the base that grade upwards to shallow platformal, tidal and supratidal facies (Dardenne, 2000). Large carbon isotopic anomalies (−4‰ to +16‰) are recorded only in the Bambuí Group (Iyer et al., 1995; Chang, 1997; Kawashita, 1998) and have been related to global post-Sturtian Neoproterozoic record (Babinski and Kaufman, 2003). The evidences for the correlation of these groups are the occurrence of similar diamictite units at the base of both groups (Dardenne, 2000), and $^{87}Sr/^{86}Sr$ signals of preserved samples from carbonate and carbonate fluorapatite of both units (Azmy et al., 2001; Misi, 2001).

Sm–Nd analyses carried out on detrital sediments from the Vazante Group indicate an uniform distribution of Sm–Nd model ages (T_{DM}) values between 1.7 and 2.1 Ga (Pimentel et al., 2001), which reflect the overlap of sources associated with the Paranoá (T_{DM}=2.0–2.3 Ga) and the Bambuí groups (T_{DM}=1.4–1.9 Ga). According to Pimentel et al. (2001), the older sources for the Vazante metasediments suggest an intermediate stratigraphic position of the Vazante Group between the Paranoá passive margin and the Bambuí Group. The tectonic setting of the Vazante Group could correspond to the upper continental passive margin deposited at ca. 900–800 Ma (Pimentel et al., 2001) or would indicate sedimentation in a rapidly subsiding basin in front of the early uplift of the Brasília Fold Belt (Dardenne, 2000).

3. The Vazante Group Zn–(Pb) deposits

3.1. The Vazante hypogene nonsulfide zinc deposit

The nonsulfide zinc mineralization is epigenetic, linked to the development of the Vazante Shear Zone (Fig. 3A), which is approximately 12 km long, strikes N50E, dips 60NW, and has been interpreted as a transpressional transcurrent fault later reactivated as a normal fault (Pinho, 1990).

The zinc ore is hosted by gray- to pink-colored dolostone with cyanobacteria mats and bird's-eyes, slate and phyllite of the Lower Pamplona Member, close to the contact with dark gray dolostone and pyrite-bearing carbonaceous slate and marl of the Upper Morro do Pinheiro Member.

Metamorphosed basic dikes occur tectonically imbricated with hydraulic breccias, hydrothermally altered dolostones and slates, and with the nonsulfide zinc ore within the Vazante Shear Zone (Monteiro, 1997; Monteiro et al., 1999; Babinski et al., 2005).

The nonsulfide zinc ore bodies are tectonically controlled mainly by antithetic faults subsidiary to the main shear zone and display pod morphology. Small sulfide-rich ore bodies are essentially composed of sphalerite and galena. Sphalerite is dark brown and remarkably homogeneous under transmitted light and has strong yellow cathodoluminescence (CL), which could be related to its high Cd (average of 8410 ppm) and low Fe (average of 0.09%) contents (Monteiro et al., 2006). Willemite is also present in the sulfide-rich ore bodies and is commonly associated with pervasive silicification along the mylonitic foliation, as part of two distinct associations: willemite+sphalerite+franklinite±zincite (without quartz) and willemite+quartz+dolomite+franklinite±barite±smithsonite (without sphalerite). These assemblages suggest the formation of willemite from sphalerite and quartz by the reaction: $2ZnS+2SiO_2+2O_2=2ZnSiO_4+S_2$, which indicates that fS_2 and fO_2 may have played an important role in the stability of this mineral assemblage (Monteiro et al., 1999, 2006).

The massive nonsulfide zinc ore, which represents the bulk of the Vazante ore, is composed mainly of coarse-grained colloform or fibrous-radiated willemite partly replaced by fine-grained willemite, both with strong green CL. Commonly, quartz, dolomite, zincite, barite, and apatite occur associated with willemite, but sulfide relicts are absent. The predominance of this ore type could also suggest hydrothermal formation of willemite from the mineralizing fluids at high fO_2/fS_2. These conditions are consistent with those experimentally predicted by Brugger et al. (2003), leading to the formation of willemite instead of sphalerite, especially at temperatures higher than 150 °C.

In the brittle–ductile or brittle structures, hematite and Zn–chlorite are also present. In general, these minerals cut the previous willemite generations and form hematite-rich nonsulfide zinc ore bodies, which are ubiquitous in the Vazante deposit. Later siderite and sphalerite veinlets cut the nonsulfide zinc ore, and are considered as related to fluctuations in the fO_2/fS_2 conditions (Monteiro, 1997; Monteiro et al., 1999).

3.2. The Ambrósia zinc deposit

The Ambrósia deposit (Monteiro, 2002; Monteiro et al., 2006) is controlled by a reverse fault (Fig. 3B), which strikes at 30° and dips 60–80° towards SE and has been displaced by a N20 trending transverse normal fault system.

The zinc ore is hosted by brecciated dolostone of the Upper Pamplona Member, which is tectonically imbricated with rhythmic carbonaceous shale, siltstone, marl, argillaceous dolostone and intraformational breccia layers with fragments of dolostone, phosphorite, and quartz in a matrix of dolomite, quartz, microcline, and plagioclase.

Relicts of sedimentary and diagenetic textures of the host dolostone include cyanobacteria mats, stromatolitic structures, irregular fenestrae and bird's-eyes. Commonly this dolostone has fine layers made of detrital minerals, such as quartz, plagioclase, and authigenic phases, mainly quartz, microcline and euhedral pyrite, in a dolomitic matrix associated with phosphatic material.

The zinc ore bodies are composed of veins and veinlets of honey-colored sphalerite, pyrite, galena, marcasite, and coarse-grained white dolomite. The first sphalerite generation was affected by mylonitization, fragmentation, corrosion, dissolution, and mobilization associated with ductile–brittle deformation. Later, light yellow-colored sphalerite and galena veins commonly cut the mylonitized sphalerite. Veins containing Fe-rich dolomite, dolomite, quartz, phyllosilicates, and apatite commonly occur in deformed zones.

The base-metal vein sulfides overprint stylolites and tectonic fractures, suggesting an epigenetic origin for the primary ore, which was later mylonitized. Later pulses of mineralizing fluids

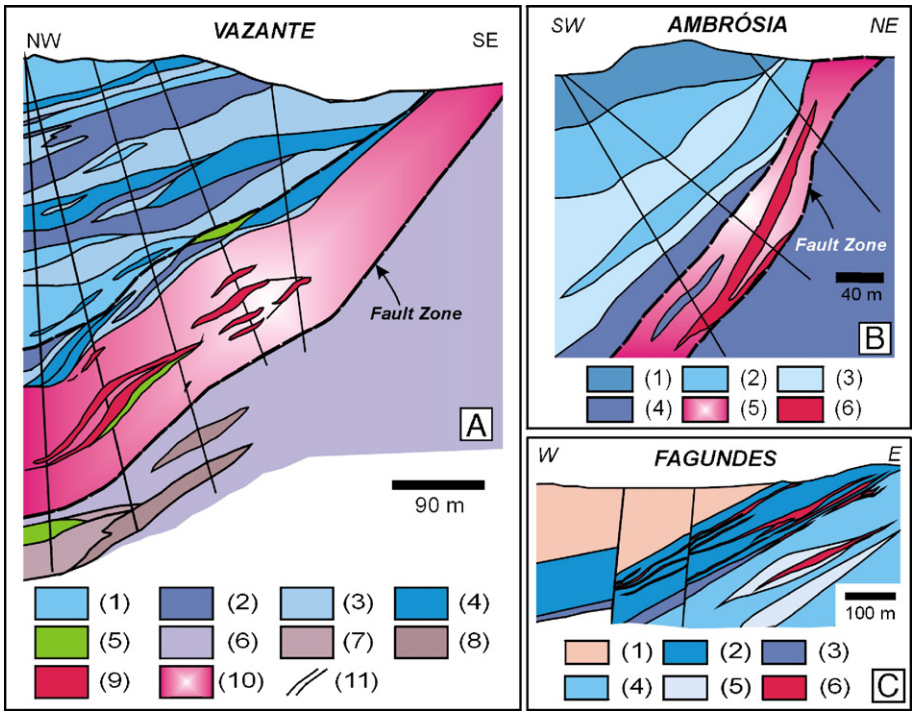

Fig. 3. (A) Cross-section of the Vazante ore zone showing the spatial relationship between host sequence, willemitic ore, and the Vazante shear zone (modified from Monteiro et al., 1999): (1–4) Serra do Poço Verde Formation, Lower Pamplona Member, (1) gray dolostone; (2) sericite phyllite; slate and metamarl; (3) pink dolostone; (4) light gray dolostone, quartz sericite phyllite, (5) metabasite; (6–8) Upper Morro do Pinheiro Member: (6) dark-gray dolostone; (7) pyrite-bearing black phyllite; (8) pyrite-rich metamarl; (9) nonsulfide zinc ore; (10) hydraulic breccias; (11) limit of the Vazante Shear Zone; (B) cross-section of the Ambrósia ore zone (Monteiro, 2002). (1–3) Morro do Calcário Formation, Upper Pamplona Member: (1) Stromatolitic bioherm; (2) gray algal-laminated dolostone; (3) light gray brecciated dolostone; (4) Serra do Poço Verde, Lower Pamplona Formation, pyrite-bearing black shale; slate, phosphatic dolostone; intraformational breccia; (5) breccia zone; (6) Zn–(Pb) mineralization; (C) cross-section of the Fagundes ore zone (Votorantim Metais). (1) Lapa Formation, Serra do Velosinho Member, Pyrite-bearing shale; (2–5) Morro do Calcário Formation, Upper Pamplona Member: (2) dolorudite with stromatolitic bioherm fragments and cyanobacteria-laminated dolostone; (3) fine-gray dolostone with green slate layers; (4) dolarenite and microcrystalline dolostone; (5) cyanobacteria-laminated dolostone; (6) Zn ore. (For interpretation of the references to colour in this figure legend, the reader is referred to the web version of this article.)

have been responsible for late sphalerite veins in the deposit. Thus, the Ambrósia deposit represents an example of hydrothermal-epigenetic mineralization, whose characteristics could reflect the evolution of the mineralizing fluid during the deformation of the host sequence related to the continuous transition between burial diagenesis and lower greenschist facies metamorphism.

3.3. The Fagundes zinc deposit

The Fagundes zinc deposit (Monteiro, 2002; Monteiro et al., 2006) is hosted by dolostones of the Upper Pamplona Member, close to the contact with rhythmic graphitic black slate of the Serra do Velosinho Member, Lapa Formation (Fig. 3C). The Upper Pamplona Member is represented in the Fagundes area by cyanobacteria-laminated dolostone, dolostone with columnar stromatolite, and dolorudite composed of a dolarenitic matrix and angular or rounded fragments of stromatolite dolostone, collophane, chert, dolomicrite, and dolomicrosparite intraclasts.

The Fagundes ore body is stratabound and the ore is composed mainly of rhythmically banded, colloform, or zoned pyrite, honey-colored sphalerite and galena. The sphalerite commonly exhibits depositional growth zoning due to oscillatory variations in minor (Fe and Cd) and trace (Ge, Cu, Ag) elements (Monteiro et al., 2006). Galena shows predominantly infilling or substitution textures, but also occurs in veins and veinlets associated with dolomite, pyrite and subordinate sphalerite. The sulfide textures of the stratabound ore indicate mainly sulfide deposition in open spaces within the dolostone host rocks, possibly related to dissolution derived from reaction with the mineralizing fluids.

Brittle–ductile and brittle processes were responsible for partial to total obliteration of the originally zoned or colloform sulfide textures, ore brecciation, mylonitization, and mobilization. Late light-yellow colored sphalerite veins and veinlets also cut the mylonitized ore zones. These late veins and veinlets could be related also to later pulses of mineralizing fluids, representing a hydrothermal-epigenetic mineralization stage, similar to those described in the Ambrósia zinc deposit.

3.4. The Morro Agudo zinc–lead deposit

The Morro Agudo deposit (Dardenne, 1979; Romagna and Costa, 1988; Oliveira, 1998; Misi et al., 1999) is hosted by breccia, dolarenitic breccia and dolarenite of the Morro do Calcário Formation (Upper Pamplona Member). The mineralized bodies are bounded by a normal fault with a strike of N170, which has been considered as a syn-sedimentary feeder zone, which acted as a preferential conduit for the metalliferous fluids

(Dardenne, 1979; Misi et al., 1999; Dardenne, 2000; Cunha et al., 2000). The ore is mainly composed of disseminated fine-grained brown-colored sphalerite and galena, with subordinated pyrite and galena. These sulfides cemented unconsolidated allochemical grains and progressively replaced diagenetically-modified coated grains. Commonly, the sulfides show convolute or compaction structures. This mineralization style has been considered mainly as syndiagenetic (Dardenne, 1979; Hitzman, 1997). Colloform sphalerite, galena, and pyrite and coarse-grained, zoned honey-colored sphalerite represent a late mineralization stage at the Morro Agudo deposit, which could be considered as late-diagenetic or epigenetic, and is similar to the main mineralization stage of the Fagundes deposit.

4. Dolomitization and diagenesis

Well-preserved diagenetic features related to multiple dolomitization events are recognized in the dolostones that occur adjacent to the ore deposits, despite the lower greenschist facies regional metamorphism that affected these rocks. The hierarchy of these dolomitization events (Fig. 4) could be useful for the recognition of the diagenetic history of the Vazante Group and to constrain the relative timing of mineralization events.

The early dolomitization event is represented by microcrystalline, replacive dolomite, preferentially developed in micrite, which comprises more than 80% vol. of the least-altered dolostones. Its origin has been considered as the result of dolomitization penecontemporaneous with the deposition of carbonate sediments in a shallow water subtidal to supratidal environment (Dardenne, 1979; Madalloso and Valle, 1978) or in a mixing-zone involving seawater and meteoric fluids (Azmy et al., 2001).

In the Lower Pamplona Member, which hosts the Vazante deposit, this early microcrystalline dolomite has been commonly recrystallized as microspar to pseudospar dolomite, due to neomorphism. Inequant (dog-tooth) and equant (blocky) spar dolomite, accompanied by quartz, commonly occur as void-filling cement (Fig. 5A), and might be related to shallow burial diagenesis, with influence of meteoric water. Fine- to medium-grained planar-s to non-planar dolomite occurs associated with stylolites (Fig. 5B). Coarse-crystalline, non-planar, non-luminescent dolomite with undulatory extinction occurs mostly as a pervasive dolomite, which obliterates any remaining texture or structure. Usually, the non-planar dolomite is accompanied by selective silicification and appears on one side of a stylolite, due to the channeling influence of stylolite. Coarse-grained saddle dolomite with curved crystal faces also occurs as fracture and vug-filling cement. Fine-grained euhedral pyrite is associated with non-planar and/or saddle dolomite and with stylolites.

In dolostones from the Upper Pamplona Member, pelleted micritic zones commonly occur associated with the early microcrystalline dolomite. Fibrous dolomite occurs locally and could represent a replacement of precursor fibrous marine cement.

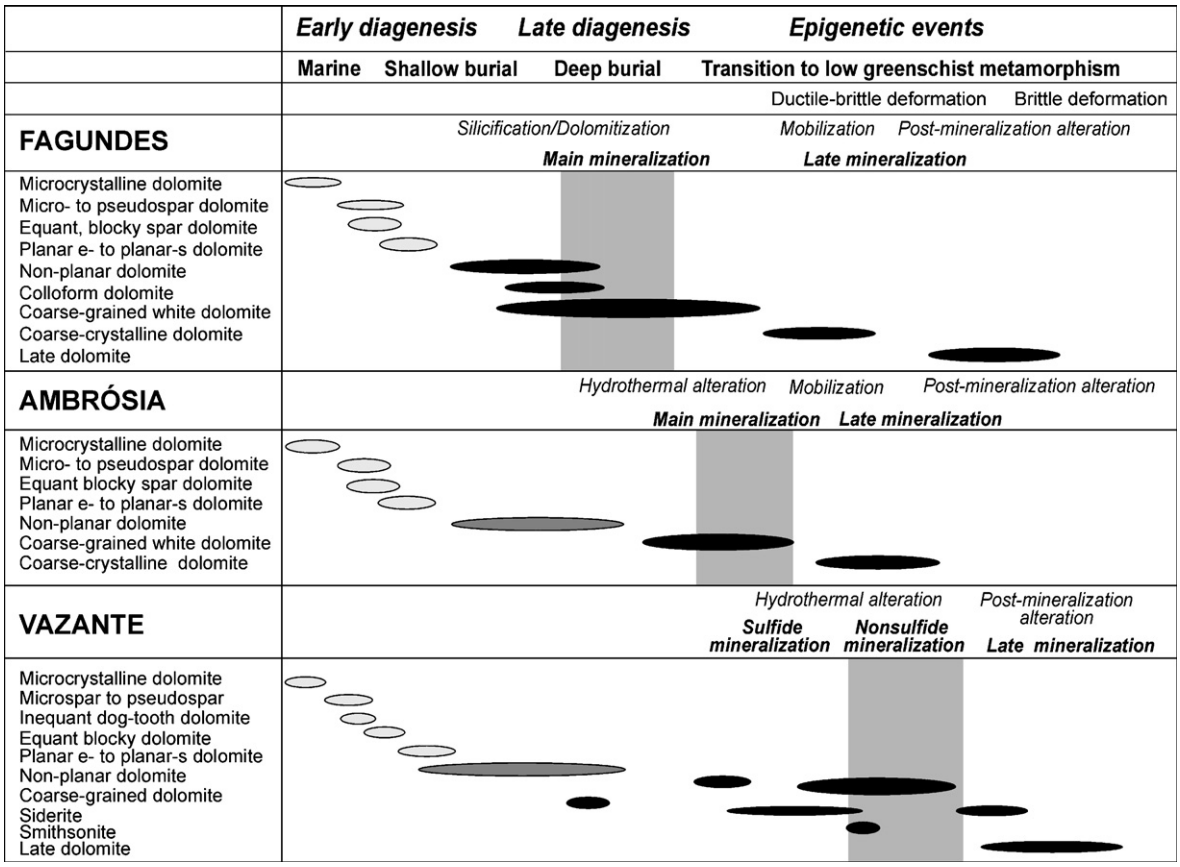

Fig. 4. Simplified paragenetic sequence of carbonate generations and relationship among dolomite generation, diagenesis and mineralization in the Vazante, Ambrósia, and Fagundes deposit. Gray rectangles represent the main mineralization stages of each deposit.

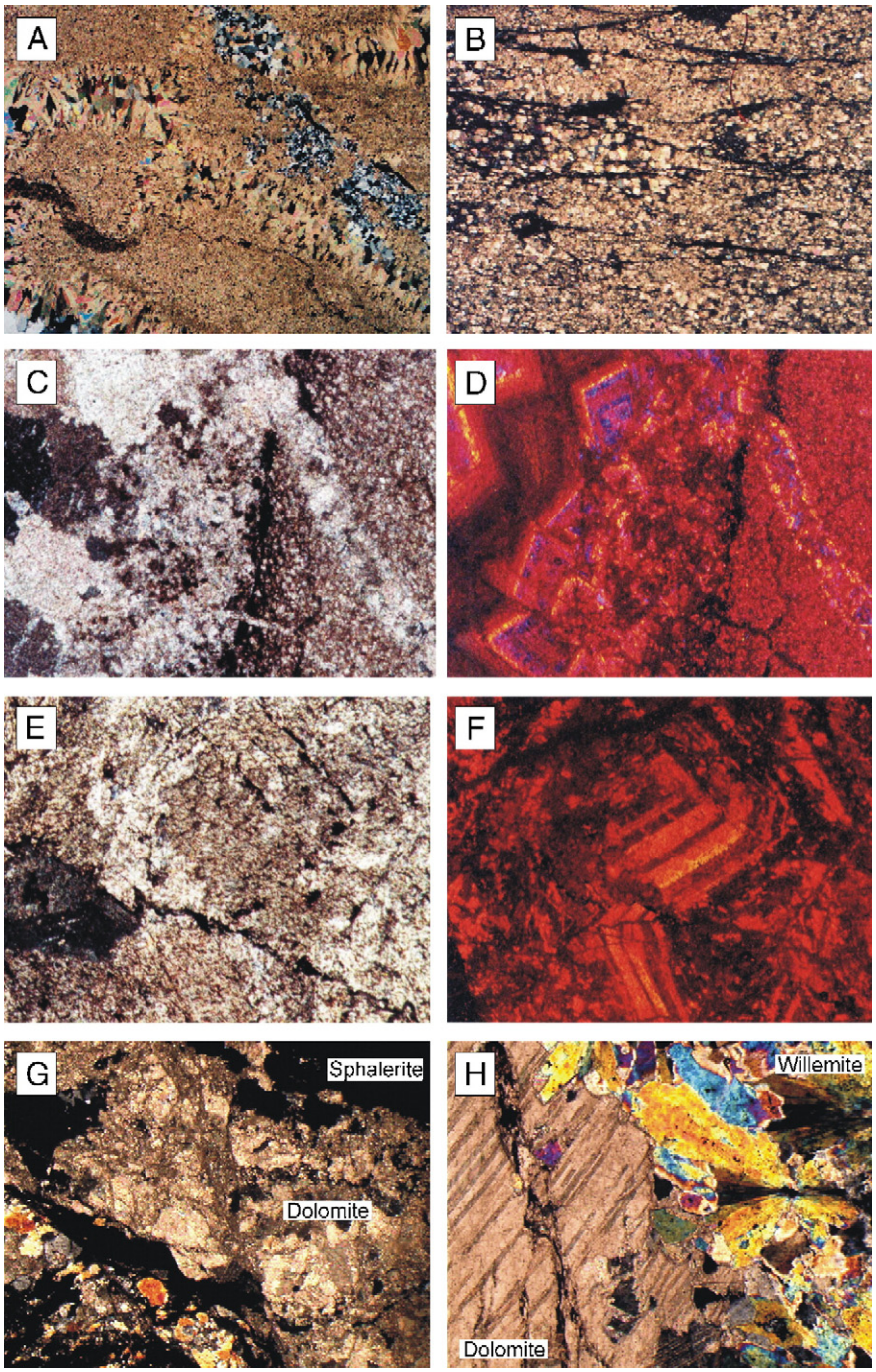

Fig. 5. Photomicrography of diagenetic and hydrothermal carbonates of the Vazante deposit. (A) Rock composed of microspar to pseudospar dolomite, with voids filled by inequant (dog-tooth) and equant (blocky) dolomite. Plane-polarized light, width of field=5.5 mm; (B) planar-s to non-planar dolomite associated with stylolites. Plane-polarized light, width of field=5.5 mm; (C) coarse-grained non-planar dolomite replacing microspar dolomite (right). Plane-polarized light, width of field=2.2 mm; (D) idem C. Cathodoluminescence zoning of coarse-grained non-planar dolomite. Light-gray zones represent bright blue CL-zones and dark-gray color corresponds to orange and red zones. Width of field=2.2 mm (E) Fractured and partially brecciated coarse-grained dolomite. Plane-polarized light, width of field=1.25 mm. (F) Idem E, showing zoning evidenced by cathodoluminescence. Different gray onalities correspond to blue, red, orange and non-luminescent CL-zones. Width of field=1.25 mm; (G) brecciated coarse-gray dolomite cut by sphalerite and galena from sulfide-rich ore bodies. Plane-polarized light, width of field=5.5 mm; (H) coarse-grained zincian dolomite (left) partially replaced by colloform willemite (right). Plane-polarized light, width of field=1.39 mm. (For interpretation of the references to colour in this figure legend, the reader is referred to the web version of this article.)

Inequant and equant, blocky spar dolomite infill fenestrae (Fig. 6A and G), and are possibly related to early diagenesis. Locally, fine- to medium-grained (<100 μm), planar-e or planar-s dolomite occurs as rhombs, and has replaced the microcrystalline dolomite (Fig. 6B). Coarse-crystalline, non-planar, non-luminescent dolomite with undulatory extinction occurs mainly as pervasive cement and appears on one side of stylolites (Fig. 6H). This later non-planar dolomite is quite similar to that recognized in dolostones from the Lower Pamplona Member and possibly indicates a similar paragenetic position, although

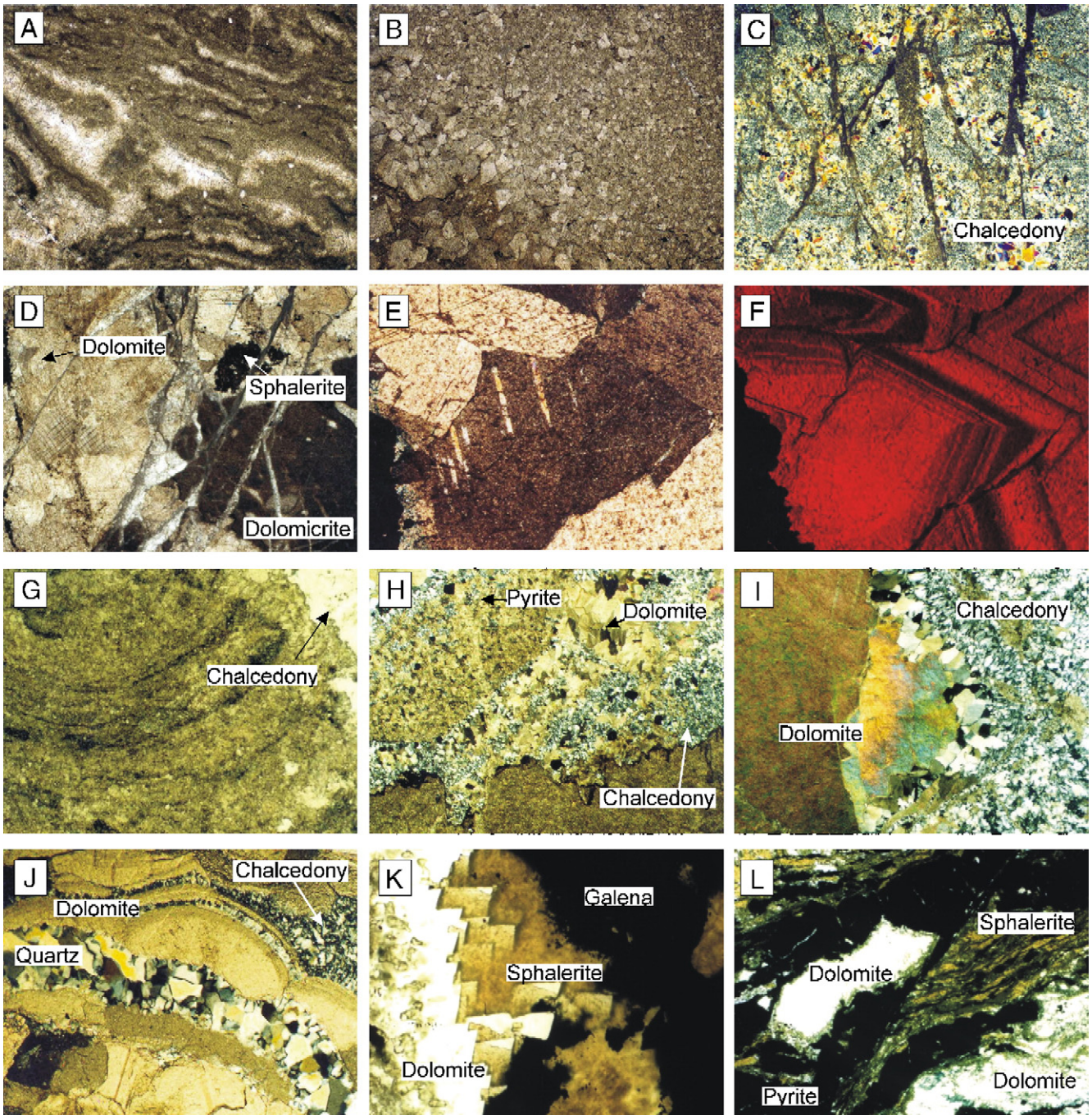

Fig. 6. (A) to (F) Photomicrography of diagenetic and hydrothermal carbonates of the Ambrósia deposit. (A) Cyanobacteria-laminated dolomicrite with fenestrae filled by inequant and equant dolomite cements. Plane-polarized light, width of field = 5.5 mm; (B) planar-e to planar-s dolomite, which occurs as rhombs and replaces the dolomicrite. Plane-polarized light, width of field = 5.5 mm; (C) silicified dolomicrite composed mainly of chalcedony and microcrystalline quartz, cut by dolomite veinlets. Plane-polarized light, width of field = 5.5 mm; (D) dolomicrite (left) replaced by coarse-grained white dolomite (right) with sphalerite associated. Dolomite veinlets cut coarse-grained dolomite and sphalerite. Arrow indicates subordinated sphalerite. Plane-polarized light, width of field = 5.5 mm; (E) coarse-grained white dolomite related to the main mineralization stage. Plane-polarized light, width of field = 5.5 mm; (F) idem E, showing zoning evidenced by cathodoluminescence. Light-gray color corresponds to bright red color and dark-gray to dull luminescence. Width of field = 5.5 mm. (G) to (L) Photomicrography of diagenetic and hydrothermal carbonates of the Fagundes deposit. (G) Preserved stromatolite dolostone affected by weak silicification (upper right). Plane-polarized light, width of field = 5.5 mm; (H) non-planar dolomite and chalcedony occur on one side of stylolite, replacing microspar to pseudospar dolomite (bottom). Pyrite appears as euhedral crystals associated with chalcedony and as fine-grained anhedral crystals in stylolite. Plane-polarized light, width of fields = 5.5 mm; (I) coarse-grained dolomite with undulatory extinction (left) associated with chalcedony (right) in strongly silicified dolostone. Plane-polarized light, width of field = 5.5 mm; (J) colloform dolomite associated with chalcedony and quartz from strongly silicified dolostone. Plane-polarized light, width of field = 1.39 mm; (K) coarse-grained zincian dolomite replaced by sphalerite. Plane-polarized light, width of field = 0.52 mm; (L) dolomite in mobilized and mylonitized ore, associated with pyrite and sphalerite. Plane-polarized light, width of field = 0.62 mm. (For interpretation of the references to colour in this figure legend, the reader is referred to the web version of this article.)

according to Wilkinson (2003), this does not imply a temporal equivalence (even if formed by a similar process) since cementation in the basin may have been diachronous. The common relationship between non-planar dolomite and stylolites might have been related to burial diagenesis.

The presence of several phases of dolomite cementation indicates a significant diagenetic history prior to the formation of non-planar dolomite in the Upper and Lower Pamplona members. Formation of this non-planar dolomite has been related to warm (120–130 °C) evolved formational waters; a knowledge that has been achieved through fluid inclusions and stable isotope studies (Azmy et al., 2001). This would also be coherent with a deep burial setting for this last diagenetic dolomitization episode observed in the Vazante Group.

5. Hydrothermal alterations

Close to the mineralized zones, the dolostones have been affected by hydrothermal alteration, commonly involving dolomite precipitation/replacement, related to focused hydrologic outflow, which occurs typically along faults and fractures.

In the Vazante deposit, the hydrothermal alteration of dolostone and slate has been largely fracture-controlled, producing a complex zone of net-veined breccia filled by dolomite, zincian dolomite, siderite, jasper, hematite, and chlorite (Monteiro, 1997; Monteiro et al., 1999). Pervasive alteration of the hanging wall dolostone of the Lower Pamplona Member is characterized by color alteration from gray or pinkish to red. This pervasive alteration is represented mainly by silicification and replacement by dolomite, siderite, jasper, hematite, and chlorite. The micritic to pseudospar dolomite, as well the spar dolomite cements, are totally recrystallized and replaced by coarse-grained (>5 mm) pinkish to red dolomite with undulatory extinction. The coarse-grained dolomite exhibits strong zoning that is documented by red, blue, yellow, orange and non-luminescent cathodoluminescence (CL) zones (Fig. 5C−F). Mylonitization fabric and brecciation of this dolomite are also commonly recognized (Fig. 5E), as well as replacement of the coarse-grained dolomite by willemite (Fig. 5F). Post-mineralization alteration comprises mainly hematite, Zn–chlorite, and dolomite. The footwall dolostone of the Upper Morro do Pinheiro Member shows initial fracture-controlled alteration, which is accompanied by color change from dark gray to pinkish around dolomite and siderite veins. This alteration style grades to pervasive style involving progressive replacement of dark gray micrite dolomite by coarse-grained dolomite and siderite, which obliterated the original texture. Along the contact with metabasite, the dolostones are strongly mylonitized, bleached, and display a mineral assemblage composed of dolomite, chrysotile, chlorite, and quartz, which is indicative of metasomatic alteration.

Locally, within the Ambrósia deposit, selective silicification of host dolostones, characterized by chalcedony and quartz replacement, occurs within the fault zone (Fig. 6C). Usually, the Ambrósia host dolomite displays recrystallization, replacement by coarse-grained dolomite (Fig. 6D) with zoning evidenced by bright red and non-luminescent CL zones (Fig. 6E and F), besides veining and faulting. Pervasively altered dolostones show color modification from gray to beige. The formation of coarse-grained dolomite occurred prior or synchronous with the main mineralization stage, but postdated burial diagenetic features, including stylolites and the non-planar dolomite, indicating that the hydrothermal alteration was mainly epigenetic. Post-mineralization alteration is represented by coarse-crystalline dolomite, talc, chlorite, and apatite and occurs mainly in mylonitized zones.

In the Fagundes deposit, silicification has been a common pre-mineralization process of open-space filling. It involved partial or total replacement of dolostones by layered chert concretions, chalcedony nodules, and mosaic quartz. Initial silicification has been associated with non-planar dolomite and stylolitic surfaces, which could indicate a relationship between silicification and burial environment (Fig. 6H). Coarse-grained (Fig. 6I) and colloform (Fig. 6J) dolomite generations usually appear in strongly silicified dolostone.

The primary mineralization postdated the burial non-planar dolomite formation and silicification; however, it was locally overprinted by chemical compaction features, such as stylolites. This could suggest a late-diagenetic to epigenetic origin for the Fagundes main mineralization. This main mineralization stage is accompanied by replacement of the dolostone by white coarse-grained dolomite with undulatory extinction. This represents a pervasive process, accompanied by color alteration from gray to a beige or pinkish tone. Colloform or rhythmic dolomite also occurs related to colloform sulfides. Textures indicative of intergrowth between coarse-grained dolomite and sphalerite and substitution of dolomite by sphalerite (Fig. 6K) are common in the Fagundes deposit. These alteration processes represent possibly more focused variants of the burial dolomitization mechanisms, as described by Warren (2000).

Epigenetic coarse-crystalline dolomite with strong undulatory extinction is also related to mobilization processes, occurring in ribbons (Fig. 6L) and late veins in the deformed zones. Late dolomite, usually euhedral, has been related to post-mineralization alteration, which comprises chlorite, quartz, and apatite.

6. Analytical methods

Oxygen and carbon isotopic analyses on whole-rock and mineral samples were conducted at the Instituto de Geociências, Universidade de São Paulo. Carbon and oxygen isotope ratios in carbonate samples were determined using the method of (McCrea, 1950). CO_2 was produced by the reaction of powdered dolomites with 100% H_3PO_4 at 25 °C for 1 to 3 days. The released CO_2 was analyzed by an Europa Geo 20–20 mass spectrometer. The uncertainties of the isotope measurements were 0.1‰. The oxygen and carbon isotope results are expressed in conventional delta (δ) notation, as per mille (‰), and were reported in relation to the Standard Mean Ocean Water (SMOW) and Pee Dee Belemnite (PDB) standards, respectively.

Mineral chemical analyses were obtained by a JEOL JXA 8600 electron microprobe at the Instituto de Geociências, Universidade de São Paulo. The wavelength dispersive technique

was employed, with accelerating voltages of 20 kV, probe current of 5 μA and beam diameter of 5 μm.

Whole-rock samples were analyzed at the Activation Laboratories Ltd., Canada, after lithium metaborate or tetraborate fusion using ICP (Inductively Coupled Plasma emission spectrometry) and INAA (Instrumental Neutron Activation Analysis). Total C, S and CO_2 were determined by combustion infrared using a LECO sulfur–carbon determinator.

Analytical data tables may be requested to the main author.

7. Results

7.1. Carbonate chemistry

Hydrothermal carbonate phases from altered and mineralized rocks of the Fagundes deposit have near stoichiometric to slightly enriched values for calcium (48.30–51.41 mol% $CaCO_3$), and low $FeCO_3$ (up to 0.69 mol%) and $MnCO_3$ (up to 0.22 mol%) contents (Fig. 7A). Dolomite from the silicified rocks has low $ZnCO_3$ contents (up to 0.08 mol%), but dolomite associated with rhythmic and colloform sulfides displays up to 3.20 mol% of $ZnCO_3$.

In the Ambrósia deposit, hydrothermal dolomite has 47.79–52.07 mol% $CaCO_3$ and 43.06–49.39 mol% $MgCO_3$, and displays higher $FeCO_3$ (up to 6.39 mol%) and $MnCO_3$ (up to 0.63 mol%) contents than those observed in the Fagundes dolomite (Fig. 7B). The highest $FeCO_3$ and $MnCO_3$ contents occur in coarse-grained white dolomite, which is associated with zinc mineralization and dolomite from mylonitized zones. The highest $ZnCO_3$ contents (up to 1.05 mol% $ZnCO_3$) occur in dolomite from mylonitized zones.

In the Vazante deposit, gangue dolomite (Fig. 7C) from sulfide-rich and nonsulfide ore bodies has 47.24–50.03 mol% $CaCO_3$. Dolomite intergrowth with sulfide at Vazante shows narrow variation of $FeCO_3$ (2.01–2.71 mol%), $MnCO_3$ (0.13–0.20 mol%) and $MgCO_3$ (46.82–48.74 mol%) contents, whereas dolomite associated with willemite reveals higher chemical variations. The highest $FeCO_3$ and $MnCO_3$ contents are found in dolomite from nonsulfide ore bodies, which also present a positive correlation between $FeCO_3$ and $SrCO_3$. Zinc incorporation in the dolomite structure is significant (up to 4.52 mol% of $ZnCO_3$) and occurs mainly in dolomite associated with willemite and hematite. Relatively high Pb (up to 0.4 mol% $PbCO_3$) and Ba (up to 0.19 mol% $BaCO_3$) contents are also verified in dolomite from the Vazante deposit.

The $FeCO_3$ and $MnCO_3$ contents of the dolomite from all these three deposits are lower than those reported by Bez (1980) for hydrothermal dolomite of the Morro Agudo deposit (Fig. 7D). In Fagundes, Ambrósia, and Morro Agudo, a positive correlation between $FeCO_3$ and $MnCO_3$ contents (correlation factor = 0.91) in dolomite may be suggested (Fig. 7D). In Vazante dolomite, however, a wide variation of $FeCO_3$ contents is accompanied by a narrow range of $MnCO_3$ values.

The incorporation of $FeCO_3$ and $MnCO_3$ in dolomite is generally promoted by reducing conditions, and would reflect the concentrations of these elements in the hydrothermal fluids, because even under disequilibria conditions their concentrations are critically dependent on the viability of the chemical species in the fluid (Savard, 1996). According to the bulk solution equilibrium theory (Veizer, 1983), Fe and Mn, which have distribution coefficients (K_D) higher than 1, should be in a relatively high concentration in dolomite near the recharge area. Thus, this could suggest proximity of the Morro Agudo deposit with outflow zones and a northward flow of Fe- and Mn-rich fluids in the Upper Pamplona Member dolostones, from the proximal Morro Agudo towards the distal Fagundes area. Alternatively, interaction with local sources of Fe and Mn during multiple flows, as previously reported by Savard (1996) for the Gays River Formation, Nova Scotia, could be also suggested.

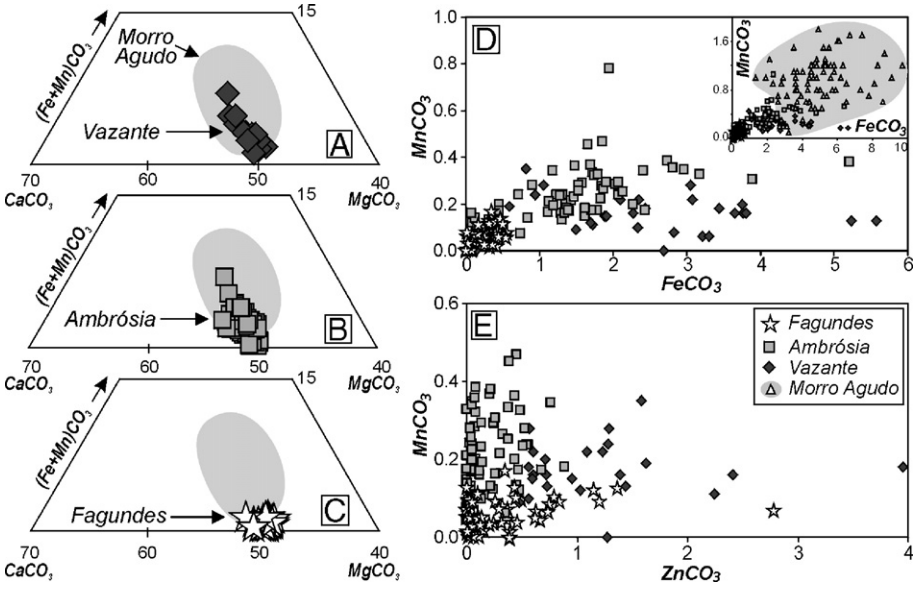

Fig. 7. (A–C) Composition of dolomite from the Vazante, Ambrósia, and Fagundes deposits in terms of $CaCO_3$–$MgCO_3$–$(Fe+Mn)CO_3$ (in mol%). (D) $FeCO_3$ versus $MnCO_3$ plot, and $ZnCO_3$ versus $MnCO_3$ diagrams showing composition of dolomite. The gray field represents the dolomite composition of the Morro Agudo deposit (Bez, 1980).

The remarkable chemical homogeneity of the Fagundes dolomite (Fig. 8A and D) could indicate the formation in an open-system, characterized by a high volume (high W/R ratio) of considerably oxidized fluids, in a similar way to those reported by Savard (1996) and Warren (2000).

The syn-ore dolomite of the Fagundes and Vazante deposits displays considerable amounts of $ZnCO_3$ (Fig. 7E), which are similar to those described to be present in zincian dolomite of the Navan Zn–Pb deposit, Ireland (Kucha and Wieczorek, 1984) and of the Beltana and Aroona willemite deposits (Groves et al., 2003; Carman, 2003).

According to Kucha and Wieczorek (1984), zincian dolomite is relatively unstable in the presence of H_2S, because reactions between zincian dolomite and H_2S result in sphalerite formation. Thus, dolomite associated with colloform sulfides of the Fagundes deposit could suggest that the metalliferous fluid is relatively sulfur-deficient. This could explain replacement textures and intergrowth of these minerals, which commonly occur in the Fagundes deposit. In the Vazante deposit, progressive consumption of sulfur from this fluid would yield early sphalerite precipitation followed by willemite deposition, explaining the paragenetic sequence observed at Vazante and in others hypogene nonsulfide zinc deposits, such as Berg Aukas, as previously proposed by Hitzman et al. (2003).

7.2. Mass balance calculations

7.2.1. Mass balance of hydrothermal alteration

Mass balance calculations were used to estimate gains and losses of chemical compounds necessary to produce the hydrothermally altered rocks within the mineralized zones of each deposit. The adopted methods were those outlined by Gresens (1967), Grant (1986), Potdevin and Marquer (1987), and Potdevin (1993), considering an open system with mass and volume variations. The mass balance between unaltered and hydrothermally altered rocks was calculated in relation to the average composition of least-altered dolostones from each deposit, considering the measured density of the analyzed samples. H^+ and O^{2-} were assumed as independent elements, as recommend by Potdevin and Marquer (1987) for hydrothermal

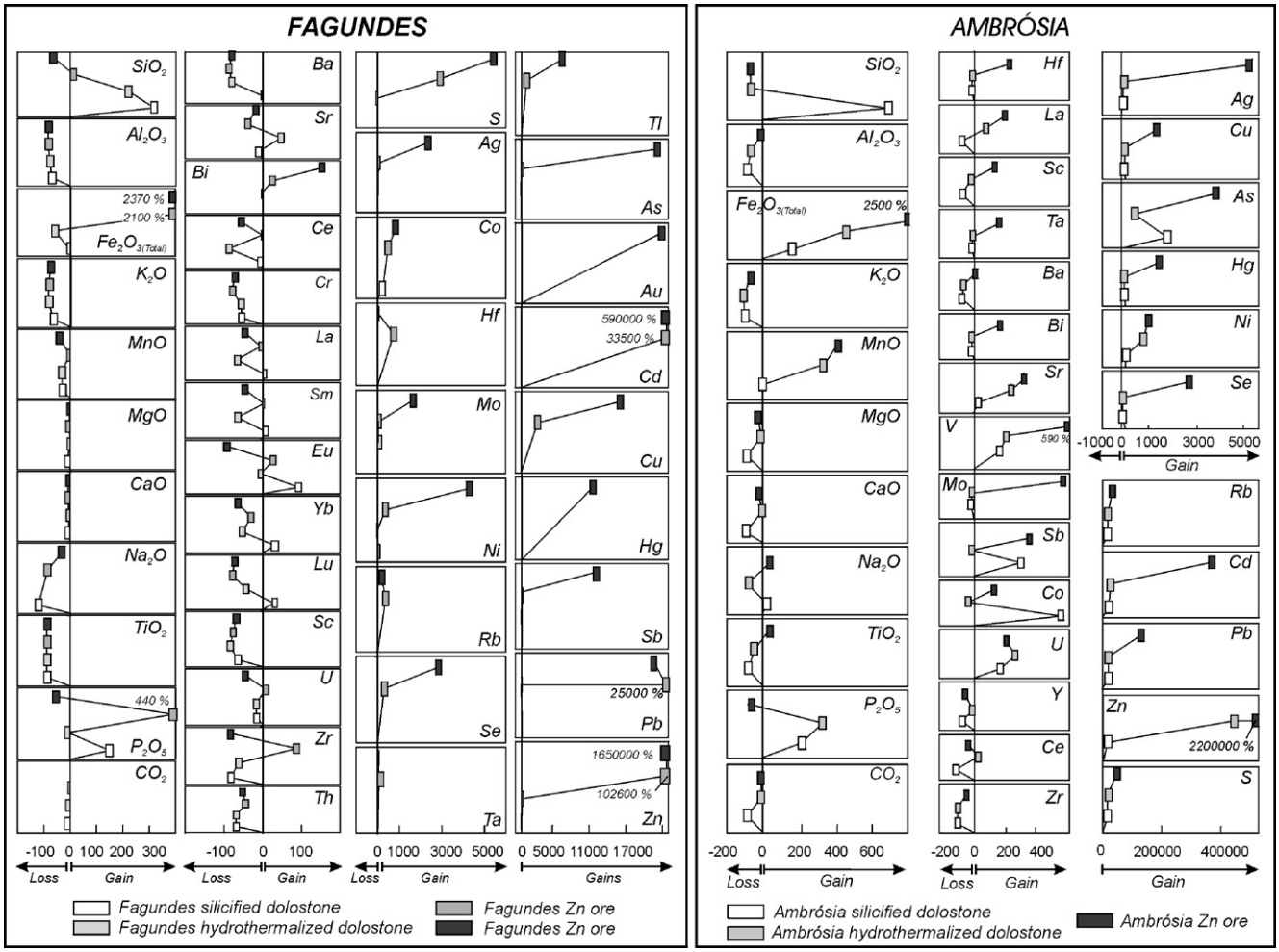

Fig. 8. Mass balance of the altered and mineralized dolostones from the Fagundes and Ambrósia deposits, considering an open system with mass and volume variations, O^{2-} as independent and immobile element, and using the average composition of the least-altered dolostone of the Upper Pamplona Member at each area for comparison, which is represented by vertical lines. Horizontal bars correspond to mass balance ranges of samples of the same alteration or mineralization style. Lines bind average compositions and indicate the evolutionary sequence of alteration and mineralization. Based on methods outlined by Gresens (1967), Grant (1986), Potdevin (1993).

systems. Diagrams of Grant (1986) and Potdevin and Marquer (1987) were used to define elements with the lowest volume valor (f_V) or relatively immobile behavior.

In the Fagundes deposit, pervasive silicification and replacement by coarse-grained white dolomite are mainly pre-mineralization processes. They have been accompanied by a relative gain of SiO_2 (up to 300% of the original SiO_2 content) and relative loss of characteristic elements of the non-carbonatic fractions, such as Al_2O_3, K_2O, MnO, Na_2O, TiO_2, Zr, Th, U, Cr, and Sc (Fig. 8; Table 1), in relation to the average composition of the least-altered dolostones from Fagundes (Fig. 9). Silicification was also accompanied by gains of P_2O_5 (up to 150% of the original P_2O_5 content), La, Sm, Eu, Yb, and Lu and a slight relative loss of Sr. In the dolostone replaced by coarse-grained dolomite occurs also loss of $Fe_2O_{3(T)}$ and increase of Sr contents.

These mass balance calculations indicate that the pre-mineralization processes, at Fagundes, were not accompanied by any significant increase in the typical elements of the sulfide mineralization, except for P_2O_5. Additionally, the relative loss of $Fe_2O_{3(T)}$ and MnO in hydrothermally altered dolostones from the Fagundes deposit could reflect relatively oxidized conditions for these early hydrothermal fluids, which are distinct from those typically predominant during the burial diagenesis and deep-seated basinal fluids (Warren, 2000).

In the Ambrósia deposit, silicification and replacement by coarse-grained white dolomite are accompanied by relative gains of $Fe_2O_{3(T)}$, P_2O_5, U, Sr, V, As, Rb, Cd, Pb, Zn, and S and relative loss in Al_2O_3, K_2O, TiO_2, Yb, Zr, La, and Th (Fig. 8; Table 1), which are mainly present in detrital phases, and in CaO, MgO, CO_2, and Ba, which could reflect carbonate dissolution processes. The silicified dolomite also shows, besides an increase of more than 600% of the original SiO_2 content, enrichment in Na_2O, Sb, and Co. The Ambrósia dolostone replaced by coarse-grained white dolomite presents a slight increase in La, Ce, Cr, and Ni contents and relative gains of 300% of Mn, which are consistent with the chemical composition of the hydrothermal dolomite from Ambrósia. These mass balance calculations might also indicate that hydrothermal alteration processes reflect interaction with Zn- and Pb-rich

Table 1
Main geochemical modifications related to hydrothermal alteration and mineralization processes

DEPOSIT	Host unit	Hydrothermal alteration/mineralization	Geochemical characteristics (mass balance)	
			Main gains	Main losses
	Upper Morro do Pinheiro Member	Fracture-controlled to pervasive alteration of the footwall dolomites, characterized by color alteration from dark gray to pinkish related to dolomite and siderite veins	SiO_2, Al_2O_3, $Fe_2O_{3\ (T)}$, MnO, (TiO_2) Zn, Pb, Cd, V, U, Co, As, Sb, Ba, Cu, Ni, Cr, La, Ce, Sc, Sm, Zr, Y	K_2O, Na_2O, P_2O5, Sr, Br, (Ag)
		Pervasive alteration of the dolomites in tectonic contact with metabasites characterized by color alteration from dark gray to white (bleached dolomites)	$Fe_2O_{3(T)}$, MnO, Na_2O Zn, Pb, Cd, V, Ba, Cu, Ni, Au, Co	SiO_2, (Al_2O_3), K_2O, P_2O5, (Ag)
Vazante	Lower Pamplona Member	Pervasive alteration of the hanging wall dolomites characterized by color alteration from gray or pinkish, associated with silicification and replacement by zincian dolomite, siderite, jasper, hematite, and chlorite.	SiO_2, $Fe_2O_{3(T)}$, MnO, TiO_2, P_2O_5 Zn, Pb, Cd, Ag, S, V, U, Co, As, Sb, Ba, Cu, Ni, Cr, Rb, La, Sm, Zr, Y	CaO, MgO, (Al_2O_3), K_2O, Na_2O, Sc, Br
		Willemitic mineralization: pods with colloform and fibrous-radiated willemite, quartz, dolomite, zincite, barite, apatite, franklinite, smithsonite, hematite, chlorite	SiO_2, $Fe_2O_{3(T)}$, TiO_2, (P_2O_5,), (MnO), (Na_2O), Zn, Pb, Cd, Ag, S, V, U, Co, As, Sb, Cu, Ni, Rb, La, Zr, Y	CaO, MgO, (Al_2O_3), K_2O, (CO_2), Sc, Sr
		Sulfide mineralization: small bodies with pale gray-colored sphalerite, galena, franklinite, quartz, siderite, dolomite	SiO_2, $Fe_2O_{3(T)}$, TiO_2, (Sc),V, Co, Zn, Pb, Cd, Ag, S, Ba, Br, Cr, As, Au, Sb, Cu, Ni, Hg, Se, Y, Sm	CaO, MgO, (MnO), Al_2O_3, K_2O, Na_2O, P_2O_5, CO_2, Sr, Zr
Ambrósia	Upper Pamplona Member	Selective silicification of host dolomites	SiO_2, $Fe_2O_{3(T)}$, P_2O_5, Na_2O, U, V, Sb, Co, As, Zn, Pb, Cd, S, Rb, Sr	Al_2O_3, K_2O, CaO, MgO, TiO_2, CO_2, La, Sc, Sm, Zr, Y, Th, Yb, Ba, Ce, Cr
		Recrystallization and replacement of the host dolomites by coarse-grained white dolomite	$Fe_2O_{3(T)}$, MnO, P_2O_5, U, V, Rb, Sr, As, Ni, Zn, Pb, Cd, S, La	Al_2O_3, K_2O, Na_2O, TiO_2, SiO_2 Zr, Y, Th, Yb, Ba
		Sulfide mineralization: veins with honey-colored sphalerite, pyrite, galena, marcasite, dolomite, quartz	$Fe_2O_{3(T)}$, MnO, Na_2O, TiO_2, Sr, Rb, Zn, Pb, Cd, Ag, S, V, U, Co, Mo, Bi, Br, As, Au, Sb, Cu, Ni, Hg, Se, Tl, Hf, La, Lu, Sc	K_2O, P_2O_5, SiO_2, Y, Yb, Zr, Ce, Cr, Eu
Fagundes	Upper Pamplona Member	Pervasive silicification related to replacement of the host dolomite by chalcedony, quartz and white dolomite	SiO_2, P_2O_5, Co, Eu, Yb, Lu	Al_2O_3, K_2O, MnO, Na_2O, TiO_2, MgO(*), CaO*, Zr, Th, Cr, Sc, U, Sr
		Aalteration of the host dolomites marked by color alteration from gray to beige, and replacement by white dolomite.	SiO_2, Sr, CaO(*), MgO(*)	Al_2O_3, $Fe_2O_{3(T)}$, K_2O, MnO, Na_2O, TiO_2, MgO(*), CaO(*), Ba, La, Ce, Sm, Zr, Yb, Th, Cr, Sc, Lu, U
		Sulfide mineralization: rhythmically banded, colloform, or zoned pyrite, honey-colored sphalerite, galena, dolomite, quartz	$Fe_2O_{3(T)}$, (P_2O_5,), Rb, Zn, Pb, Cd, Ag, S, Co, As, Au, Sb, Cu, Ni, Hg, Se, Mo, Hf	SiO_2, Al_2O_3, TiO_2, K_2O, MnO, Na_2O, MgO, CaO, Ba, La, Ce, Sm, Sr, Th, Sc, Lu, U, Cr, Yb

(*) indicates elements with small relative gain or loss. ( ) denotes elements with a wide variation interval.
Mass balance calculations are based on Gresens (1967), Grant (1986),and Potdevin (1993).

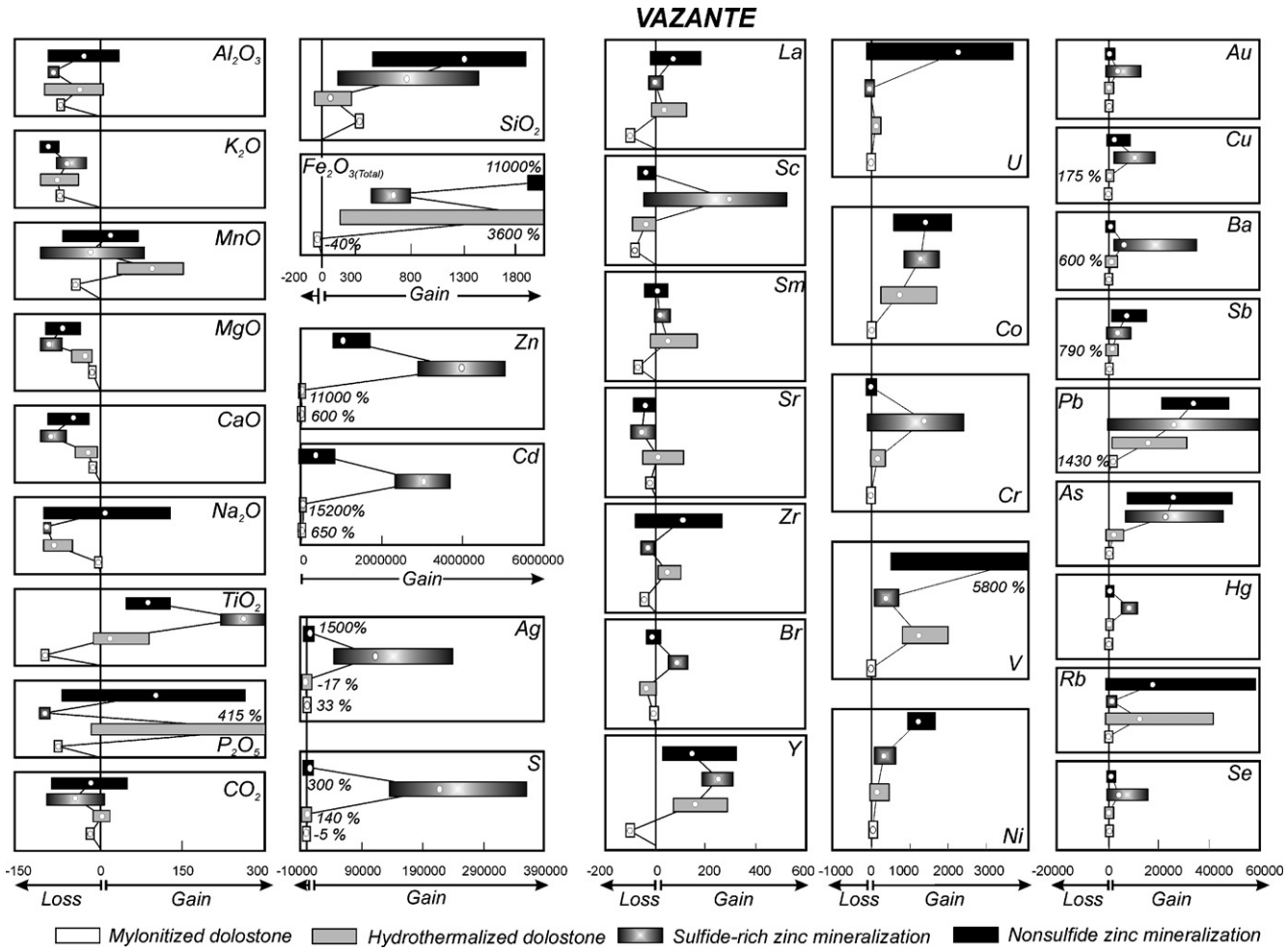

Fig. 9. Mass balance of the altered and mineralized dolostones of the Lower Pamplona Member considering an open system with mass and volume variations, O^{2-} as independent and immobile element, and using the average composition of the least-altered dolostone of the Lower Pamplona Member for comparison, which is represented by vertical lines. Horizontal bars correspond to mass balance ranges of samples of the same alteration or mineralization style. Lines bind average compositions and indicate the evolutionary sequence of alteration and mineralization. Based on methods outlined by Gresens (1967), Grant (1986), and Potdevin (1993).

fluids similar to those responsible for the epigenetic sulfide mineralization at Ambrósia.

At the Vazante deposit, within the Vazante Shear Zone, the hydrothermally altered dolostones of the Lower Pamplona and Upper Morro do Pinheiro members show a strong gain in SiO_2, $Fe_2O_{3(T)}$, MnO, P_2O_5, TiO_2, Zn, Pb, Cd, V, U, Co, As, Sb, Ba, Cu, S, Rb, Ni, Cr, La, Sm, Zr, and Y (Fig. 9; Table 1) and relative loss of K_2O, Na_2O, Al_2O_3, CaO, MgO, Sc, and Br, in relation to least-altered dolostones. The bleached dolostones, which occur in tectonic contact with metabasite within the Vazante Shear Zone, show relative gains of $Fe_2O_{3(T)}$, MnO, Na_2O, Zn, Pb, Cd, V, Ba, Cu, Ni, and Co and important losses of SiO_2, K_2O, and P_2O_5 (Table 1). Mass balance calculations (Monteiro, 1997) indicate that the mylonitized metabasite within the Vazante Shear Zone displays mass increase (3%) relative to the least-mylonitized metabasite. This mass increase is related mainly with MgO (~60%), CO_2 (~60%), Pb (~174%), and Zn (~212%) enrichments. Relative loss of Fe_2O_3 (~33%), Ba, and Sr (~60%) are also observed.

These calculations indicate that all host rocks at the Vazante deposit were intensely affected by metasomatic processes related to Zn- and Pb-rich fluids circulation within the Vazante Shear Zone.

7.2.2. Mass balance of the zinc mineralizations

Sulfide-rich zinc ore samples from the Vazante, Ambrósia and Fagundes deposits show relative gains of $Fe_2O_{3(T)}$, Zn, Pb, Cd, Ag, S, As, Sb, Au, Hg, Se, Co, Cu, and Ni (Table 1), if compared with the least-altered dolostones of each deposit. Hypogene nonsulfide zinc ore of Vazante shows strong gains of $Fe_2O_{3(T)}$, Rb, Sb, V, U, SiO_2, and La (Fig. 9; Table 1). Other elements, such as Zn, Pb, Cd, Ag, S, Co, Sb, Cu, Ni, As, and Y, which are typical of the sulfide mineralization, represent important gains in these samples, in relation to the least-altered dolostones.

The mineralizing processes in the three deposits are accompanied by losses in K_2O, CaO, and MgO (Table 1). In the Fagundes deposit relative loss in SiO_2, Al_2O_3, TiO_2, MnO, and Na_2O occurs, whereas in Ambrósia and Vazante losses of P_2O_5 and SiO_2 and of Al_2O_3, Na_2O, P_2O_5, and MnO, respectively, are observed. Strong Sr loss is also verified in the Vazante and Fagundes deposits.

The gains in similar components for all sulfide-rich ore bodies from distinct deposits suggest a common geochemical signature, which might be associated with the regional role of metal-bearing brines derived from a similar source.

7.3. Oxygen and carbon stable isotope

7.3.1. Least-altered dolostones

In the Ambrósia area, the least-altered dolostones of the Upper Pamplona Member, composed mainly of microcrystalline dolomite, display the highest $\delta^{18}O$ (29.7 to 28.6‰) and $\delta^{13}C$ (0.3 to 0.7‰) values, whereas at Fagundes the $\delta^{18}O$ (25.8‰) and $\delta^{13}C$ (−1.3‰) values are lower. The least-altered dolostones of the Lower Pamplona Member, which hosts the Vazante deposit, have $\delta^{18}O$ (26.2 to 27.7‰) and $\delta^{13}C$ (2.2 to 2.7‰) values (Monteiro, 1997; Monteiro et al., 1999).

Although the oxygen isotope composition of dolostones are most likely to reflect pore fluid composition and the temperature of dolomitization (Hoefs, 2004), the $\delta^{18}O$ values of these least-altered rocks are consistent with those of marine carbonates. Variations in the $\delta^{18}O$ values for the least-altered rocks of the Lower and Upper Pamplona members might be related to temperature variations or hypersalinity associated with the early dolomitization process, which has been considered as penecontemporaneous to sedimentation (Dardenne, 1979). Higher temperature conditions and/or deposition in an evaporitic environment would explain the highest $\delta^{18}O$ values observed in the Upper Pamplona dolostones at Ambrósia. This is consistent with the evaporite evidences in the Upper Pamplona Member described by Misi et al. (2005). The lowest $\delta^{18}O$ value from the Fagundes dolostone could reflect post-depositional processes produced by an effective hydrothermal system associated with high water/rock ratios.

Carbon isotope composition of dolostones is determined by the precursor carbonate composition. The $\delta^{13}C$ values in these least-altered rocks (−1.3 to 2.7‰) are close to those typical of marine signatures (0 to 3‰; Hoefs, 2004). The lowest $\delta^{13}C$ values (−1.3‰) from the Fagundes area might reflect variable degree of oxidation of organic matter and/or bacterial sulfate reduction processes (Burns et al., 1988), which could accompany alteration processes.

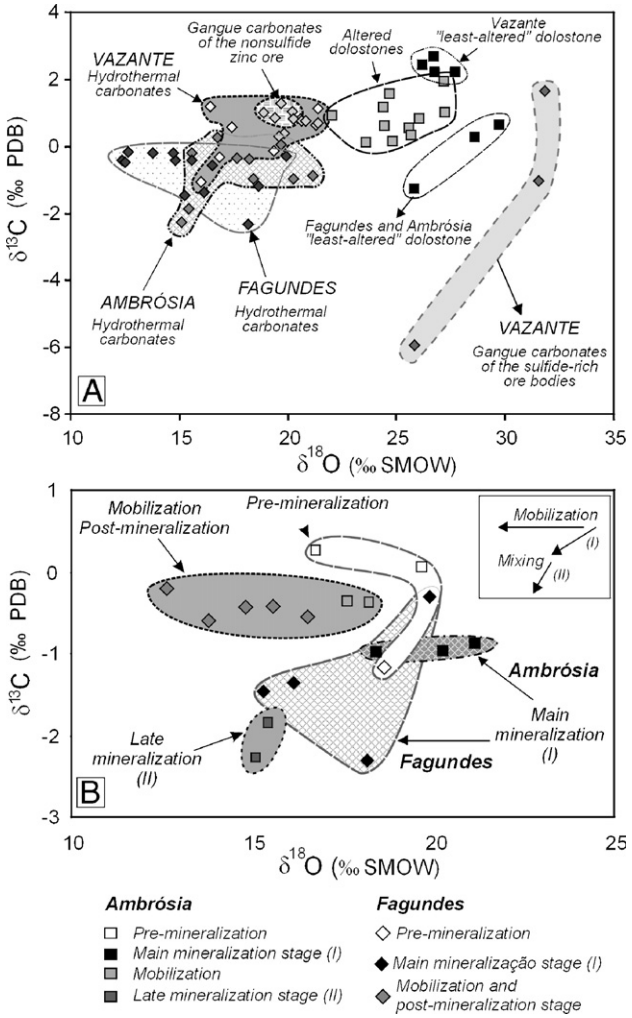

Fig. 10. (A) Oxygen and carbon isotopic composition of least-altered and altered dolostones and hydrothermal carbonates from the Vazante, Ambrósia, and Fagundes zinc deposits; (B) oxygen and carbon isotopic composition of the hydrothermal carbonates of the Ambrósia and Fagundes zinc deposits, showing two covariant trends related with mobilization involving meteoric fluids and mixing processes, respectively.

7.3.2. Hydrothermally altered host rocks

The hydrothermally altered dolostone of the Vazante deposit exhibits a strong covariant trend characterized by decrease of $\delta^{18}O$ and $\delta^{13}C$ values (Monteiro, 1997; Monteiro et al., 1999). In the Ambrósia deposit, a decrease of $\delta^{18}O$ values (26.1 to 24.8‰) is accompanied by slight variation of $\delta^{13}C$ values (0.8 to 0.1‰) in the altered dolostones. In Fagundes, hydrothermally altered dolostones display $\delta^{18}O$ values (25.7 to 23.6‰) close to or lower than those of the least-altered dolostones, but the $\delta^{13}C$ values (1.2 to 0.3‰) are higher than those of the least-altered rocks. The decrease of $\delta^{18}O$ values observed in hydrothermally altered dolostones from Ambrósia and Vazante reflect the interaction with the hydrothermal fluids at relatively high temperatures. However, the narrow range of $\delta^{18}O$ values in hydrothermally altered dolostones at Fagundes could result from homogenization of the oxygen isotopic compositions, which are usually sensitive to hydrothermal alteration processes, due to high water/rock ratios.

7.3.3. Hydrothermal dolomite

The $\delta^{18}O$ (21.6 to 31.8‰) and $\delta^{13}C$ (−5.9 to 1.7‰) values of the gangue carbonate intergrown with sulfides at Vazante are quite different from those of the willemitic ore ($\delta^{18}O$=17.4 to 20.4‰; $\delta^{13}C$=0.3‰ to 0.9‰) and carbonate intergrown with sulfides at the sulfide-rich deposits ($\delta^{18}O$=12.4 to 20.3‰; $\delta^{13}C$=−2.3 to 0.3‰; Fig. 10A). This indicate two different covariant trends for the Vazante carbonates (Monteiro, 1997; Monteiro et al., 1999) and a partial overlap of the isotopic compositions of carbonates associated with the willemitic ore and those from Fagundes and Ambrósia deposits.

The distinct $\delta^{18}O$ and $\delta^{13}C$ covariant trend observed in carbonates related to sulfide-rich zinc ore of the Vazante deposit was interpreted, based on the models of Zheng and Hoefs (1993), as related to fluid–rock interaction (Monteiro, 1997; Monteiro et al., 1999). The involved fluid was hot (~300 °C), relatively ^{18}O-enriched (~10‰), had an initial $\delta^{13}C$ composition of −7‰ (Monteiro, 1997; Monteiro et al., 1999). The interaction between this metalliferous fluid with the host dolostones decreased the fluid temperature, promoting sulfide deposition, and increased the $\delta^{18}O$ of the fluid, consequently resulting in the heavy isotopic signatures of the gangue dolomite associated with the Vazante sulfide-rich ore.

Modeling of the $\delta^{18}O$ and $\delta^{13}C$ covariations in carbonates associated with willemite, according to Zheng and Hoefs (1993), indicate that fluid mixing processes involving the regional metalliferous fluid with isotopically light oxidizing meteoric water, might best fit the observed $\delta^{18}O$ and $\delta^{13}C$ of hydrothermal gangue carbonates related to the nonsulfide zinc mineralization.

Two evolutionary trends (Fig. 10B) were defined for the different carbonate generations of the Ambrósia and Fagundes deposits. The first trend is characterized by a decrease of $\delta^{18}O$ and $\delta^{13}C$ from early hydrothermal alteration and main mineralization to late epigenetic fracture-controlled mineralization of each deposit. The second one is associated to mobilization of the Fagundes and Ambrósia ore and post-mineralization pervasive alteration of Fagundes, and is characterized by a decrease of $\delta^{18}O$ values without significant $\delta^{13}C$ variation (Fig. 10B).

The calculated $\delta^{18}O_{H_2O}$ values, at 250 °C, for the fluids in equilibrium with dolomite from the main mineralization stage of Fagundes (9.1 to 12.5‰) and Ambrósia (11.0 to 13.8‰) are considerably lighter than those calculated from the dolomite of the Vazante sulfide-rich ore bodies (18.5 to 24.2‰), at the same temperature, using the equation of Golyshev et al. (1981).

However, these oxygen isotopic compositions are close to that predicted for the initial metalliferous fluid before an extensive interaction with the host dolostones took place. This might suggest involvement of similar metalliferous fluid in the genesis of all these deposits. However, in contrast with the Vazante sulfide-ore bodies, only limited fluid–rock interaction occurred during the fluid evolution at Fagundes and Ambrósia deposits.

Mixing processes are also likely to explain the isotopic variation observed in the Fagundes and Ambrósia deposits.

In Fagundes, evolved meteoric fluids might represent an important role in pre-mineralization alteration processes. However, strong ^{18}O-impoverishment tendency that may be attributed to meteoric fluids participation is mainly related to mobilization processes in the Ambrósia and Fagundes deposits (Fig. 10B).

Besides the meteoric water contribution, the trend characterized by decrease of $\delta^{18}O$ and $\delta^{13}C$ from early hydrothermal alteration and main mineralization to late epigenetic mineralization from Fagundes and Ambrósia carbonates might suggest mixing processes involving the metalliferous fluid and an third fluid component relatively depleted in ^{13}C, which is predominant in the Ambrósia late mineralization. This carbon isotope signature could reflect higher organic matter content in the fluid source, which could represent a potential source of sulfur supply. As the metalliferous fluid is relatively sulfur-deficient, this sulfur supply could be of fundamental importance for the genesis of the sulfide-rich deposits in the district.

8. Discussions

8.1. Hydrothermal alteration processes

Hydrothermal alterations are recognized around all the zinc-(lead) deposits hosted by the Vazante Group and commonly involved silicification and precipitation of coarse-grained white dolomite generations, which are typical of the sulfide-rich zinc deposits.

In the late-diagenetic to epigenetic Fagundes deposit, hydrothermal alteration was a pre-mineralization process that may have had a major role in the ground preparation of favorable zones for fluid migration, but do not reflect direct interaction with the metalliferous fluids. Mass balance calculations, which indicate relative loss of $Fe_2O_{3(T)}$ and MnO in hydrothermally altered dolostones, homogenization of $\delta^{18}O$ values in these altered rocks, and the chemical homogeneity of hydrothermal dolomite suggest that alteration processes in the Fagundes deposit were more likely to be linked to pre- and probably also post-mineralization interaction with oxidized warm, non-metalliferous meteoric-derived fluids, at high water/rock ratios.

Within the epigenetic structure-controlled Ambrósia deposit, the geochemistry signature of the hydrothermally altered dolostones could reflect interaction with hydrothermal fluids similar to those responsible for the sulfide mineralization at Ambrósia.

The Vazante nonsulfide zinc deposit is characterized by a distinct and strongest fracture-controlled to pervasive hydrothermal alteration represented by silicification and dolostone replacement by dolomite, siderite, hematite, jasper, and chlorite. Pervasively altered rocks have similar geochemical signature to that of the nonsulfide zinc mineralization, characterized by strong relative gains of Zn, V, U, Rb, La, $Fe_2O_{3(T)}$, and P_2O_5. Remarkable gains in U, V, and La indicate that the willemitic mineralization was accompanied by influx of strongly oxidized fluids, which might represent modified meteoric fluids, as previously proposed by Monteiro (1997) and Monteiro et al. (1999). Oxygen and carbon isotopic compositions of the hydrothermally altered rocks at Vazante reveal an alteration halo around the mineralized zones and may be useful for mineral exploration of nonsulfide zinc deposits.

8.2. Regional hydrothermal systems

Despite the differences in mineralization styles, the genesis of the deposits hosted by the Vazante Group, have been associated, based on fluid inclusion and stable isotope studies, with the regional migration of a high-temperature (>250 °C), moderate salinity, metalliferous fluid (Misi et al., 1999; Cunha et al., 2000; Monteiro, 2002; Monteiro et al., 1999, 2006; Misi et al., 2005).

Mass balance calculations indicate a similar association of $Fe_2O_{3(T)}$, Zn, Pb, Cd, Ag, S, As, Sb, Au, Hg, Se, Co, Cu, and Ni for all sulfide-rich ore bodies in the studied deposits. This signature could reflect a common source for the metalliferous fluid involved in the genesis of the Vazante–Paracatu deposits, possibly derived from the underlying basin fill, which comprise clastic metasediments and organic matter-rich pelitic units. Similar Pb isotopic signatures of galena from Vazante and Morro Agudo and hydrothermal titanite from Vazante are also diagnostic of a common lead source for both nonsulfide and sulfide zinc deposits in the Vazante–Paracatu district (Cunha et al., 2003; Misi et al., 2005; Babinski et al., 2005).

This metalliferous fluid probably interacted with different local sources of Fe and Mn, explaining the Fe–Mn concentrations of mineralization-related dolomite from different deposits, but the proximity of the Morro Agudo deposit with discharge areas could also be suggested.

The metalliferous fluid would be possibly sulfur-deficient. Evidences of a low content of reduced sulfur in the regional brine are supported by the presence of zincian dolomite, which is unstable in presence of H_2S, associated with early mineralization stages at Fagundes and with the nonsulfide mineralization at Vazante, and low Zn/Cd ratios in sphalerite from these deposits (Monteiro et al., 2006). This implies in a fundamental importance of an additional sulfur supply for the genesis of the sulfide-rich deposits in the district, which might be associated

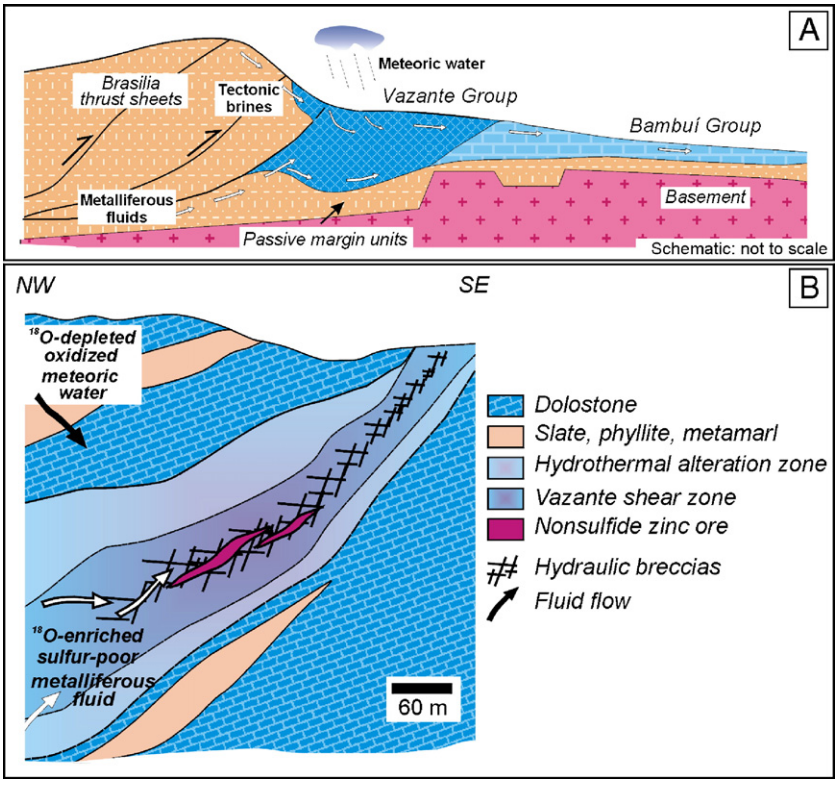

Fig. 11. (A) Schematic model of fluid flux flow in the Vazante basin, showing the interplay of meteoric waters and tectonically expelled fluids; (B) schematic model of fluid flow in the Vazante nonsulfide deposit.

with progressive mixing with sulfur-rich, saline hydrothermal fluids, as suggested by Monteiro et al. (2006). This is also consistent with the oxygen and carbon isotopic covariant trend observed for gangue carbonates of the main and late mineralization stages of the Fagundes and Ambrósia deposits.

8.3. Fluid flow and mineralization in the Vazante–Paracatu district

Different diagenetic to epigenetic mineralization styles are recognized in the Vazante–Paracatu district, which might be controlled by local stress conditions. According to Le Huray et al. (1987), the extensional regimes favor syngenetic end-member styles of mineralization, whereas compressional regimes are most likely to favor epigenetic styles in carbonate-hosted deposits. Initial mineralization in the Vazante–Paracatu district took place during the development of the extensional processes that have been active during the major period of sedimentation (Misi et al., 2005). Syndiagenetic styles of mineralization, such as those of the Morro Agudo deposit, have been related to syn-sedimentary normal faults (Dardenne, 1979, 2000), which are interpreted as feeder zones for the ascending metalliferous fluids (Misi et al., 1999; Cunha et al., 2000).

Epigenetic styles of mineralization and mobilization of pre-existing ore related to brittle–ductile structures, which are ubiquitous in all deposits in the district, are most likely linked to compressional tectonic related to the final closure of the ocean basin during the late Brasiliano orogeny (630–610 Ma; Dardenne, 2000).

According to Warren (2000), compressional tectonics, thrust faulting and extensive fracturing of carbonate strata may have been related to episodic fluid flow in response to tectonic loading. Hot (100 to >250 °C), saline and highly pressured fluids could have moved laterally out of the collision zone, typically towards the craton through permeable horizons and vertically through faults and fractures (Oliver, 1986). This compressional event could have permitted periodic expulsion of ascending metalliferous fluids and the progressive influx of tectonic brines derived from the overlying reduced shale sequences during the Brasiliano orogeny (Fig. 11A). These tectonic brines could represent an additional sulfur supply of fundamental importance for the sulfide-rich deposits in the district, besides local sulfur sources derived from evaporites, as proposed by Misi et al. (2005) for the syndiagenetic Morro Agudo deposit.

Similar hydrothermal processes, related to fluids tectonically expelled during compressive stages of the Pan African–Brasiliano Orogeny, have also been considered responsible for the genesis of the Kabwe and Kipushi lead–zinc deposits in Zambia (Kampunzu et al., 1998; Kamona et al., 1999) and Tsumeb-type Zn–Pb–(Cu) deposits in the Otavi Mountain Land, Namibia (Pirajno and Joubert, 1993; Chetty and Frimmel, 2000; Frimmel et al., 2004).

Additionally, compressive regime might have also favored infiltration of meteoric water, which was involved in: (i) ground preparation processes (e.g. Fagundes deposit); (ii) mobilization processes in the sulfide-rich deposits; and in (iii) the epigenetic nonsulfide zinc mineralization process, in which the overall mixture between the sulfur-poor metalliferous fluid and meteoric fluids, channeled to the Vazante Shear Zone (Fig. 11B), enable the high fO_2/fS_2 conditions responsible for the stability of the Vazante willemitic assemblage.

Flux of descending meteoric water would be driven by gravity from the hydrologic head established by the compressive tectonic regime (Fig. 11), similar to that modeled by Garven and Freeze (1984) and Oliver (1986) to explain the fluid flow in Mississippi-Valley type deposits.

9. Conclusions

Despite the differences in mineralogy, alteration styles, ore controls, and textures, the zinc deposits in the Vazante–Paracatu district might be associated with the regional migration of a common high-temperature (~250 °C), sulfur-poor metalliferous fluid with a geochemical signature of $Fe_2O_{3(T)}$, Zn, Pb, Cd, Ag, S, As, Sb, Au, Hg, Se, Co, Cu, and Ni. Local controls on stress and physicochemical conditions, besides the sulfur supply related with episodic expulsion of tectonic brines would have resulted in the different ore types observed in the district.

Syndiagenetic styles of mineralization, such as in the Morro Agudo deposit, could be favored by extensional tectonic. Chemistry of dolomite from Morro Agudo indicates proximity with discharge areas, possibly related with feeder zones. Epigenetic styles of mineralization (e.g. Ambrósia and Vazante) and mobilization of preexisting ore related to brittle–ductile structures, are most likely related with the inversion from extensional to compressional tectonic, during late Brasiliano orogeny. The compressional tectonic regime favored the progressive influx of tectonic brines derived from the overlying reduced shale sequences, which would represent an additional sulfur supply of fundamental importance for the sulfide-rich deposits in the district, besides local sulfur sources derived from evaporites. The lack of reduced sequences above the Vazante deposit could represent a limiting factor for H_2S supply, favoring conditions of low fS_2 responsible for the willemite stability. The compressive regime might have also favored migration of meteoric water driven by gravity from the thrust belt. The contribution of modified meteoric water has been linked with mobilization processes in the sulfide-rich deposits and was fundamental for the genesis of the Vazante nonsulfide zinc deposit.

Acknowledgments

We are very grateful to Votorantim Metais (Companhia Mineira de Metais) for allowing access to the mine, providing logistical support and much of the geological groundwork for this study.

We would especially like to thank Aroldo Misi, Fred Kamona, Gregor Borg, Jacques Cailteux, and M. Santosh, whose critical comments and useful suggestions significantly improved the paper.

Special thanks are due to Luiz Paulo B. Ribeiro and Marcos Monsueto from the Instituto de Geociências, Universidade de

São Paulo, who provided the stable isotope and microprobe analyses, respectively.

The financial support was provided by Fundação de Amparo à Pesquisa do Estado de São Paulo, Brazil (Research Grant 96/3941-3 and Doctorate Scholarship 98/0412-5), which we acknowledge with appreciation. This study is a contribution to the IGCP 450 - Proterozoic Sediment-hosted Base Metal Deposits of Western Gondwana.

References

Almeida, F.F.M., 1967. Origem e evolução da plataforma brasileira. Boletim do Departamento Nacional Produção Mineral, Brazil 243, 1–36.

Amaral, G., 1968. Geologia e depósitos de minério na região de Vazante, Estado de Minas Gerais. Ph.D. thesis, Escola Politécnica, Universidade de São Paulo, Brazil.

Azmy, K., Veizer, J., Misi, A., Oliveira, T.F., Sanches, A.L., Dardenne, M.A., 2001. Dolomitization and isotope stratigraphy of the Vazante Formation, São Francisco Basin, Brazil. Precambrian Research 112, 303–329.

Babinski, M., Kaufman, A.J., 2003. First direct dating of a Neoproterozoic post-glacial cap carbonate. 4th South Am. Symp. Isotope Geol., Salvador, Brazil. Short Papers, pp. 321–323.

Babinski, M., Monteiro, L.V.S., Fetter, A.H., Bettencourt, J.S., Oliveira, T.F., 2005. Isotope geochemistry of the mafic dikes from the Vazante nonsulfide zinc deposit Brazil. Journal of South American Earth Sciences 18, 193–204.

Bez, L., 1980. Evolução mineralógica e geoquímica do depósito de zinco e chumbo de Morro Agudo, Paracatu, MG. 31st Congresso Brasileiro de Geologia, Balneário de Camburiú, vol. 3, pp. 1402–1416.

Brugger, J., McPhail, D.C., Wallace, M., Waters, J., 2003. Formation of willemite in hydrothermal environments. Economic Geology 98, 819–836.

Burns, S.J., Baker, P.A., Showers, W.J., 1988. The factors controlling the formation and chemistry of dolomite in organic-rich sediments, Miocene Drakes Bay Formation, California. In: Shukla, V., Baker, P.A. (Eds.), Sedimentology and Geochemistry of Dolostones. Special Publication, Society of Economic Paleontologists and Mineralogists, vol. 43, pp. 41–52.

Carman, C.E., 2003. The Aroona Willemite Trend, North Flinders Ranges, South Australia: Sedimentary, Structural, and Economic Geology. Master thesis. Colorado School of Mines.

Chang, H.K., 1997. Isótopos Estáveis (C, H, O) e $^{87}Sr/^{86}Sr$: Implicações na estratigrafia e na paleo-circulação de fluidos na Bacia do São Francisco. Tese Livre-Docência, Instituto de Geociências e Ciências Exatas, Universidade Estadual Paulista.

Chetty, D., Frimmel, H.E., 2000. The role of evaporites in the genesis of base metal sulfide mineralization in the Northern Platform of the Pan-African Damara Belt, Namibia: geochemical and fluid inclusion evidence from carbonate wall rock alteration. Mineralium Deposita 35, 364–376.

Cloud, P.E., Dardenne, M.A., 1973. Proterozoic age of the Bambuí Group in Brazil. Geological Society of America Bulletin 84, 1673–1676.

Cunha, I.A., Coelho, C.E.S., Misi, A., 2000. Fluid inclusion study of the Morro Agudo Pb–Zn deposit, Minas Gerais, Brazil. Revista Brasileira de Geociências 30, 318–321.

Cunha, I.A., Babinski, M., Misi, A., 2003. Pb isotopic constraints on the mineralization from the Vazante Group, Minas Gerais, Brazil. 4th South American Symposium on Isotope Geology, Salvador, Brazil. Short Papers, pp. 727–730.

Dardenne, M.A., 1979. Les minéralisations plomb-zinc du Groupe Bambui et leur contexte géologique. Ph.D. thesis, Université Pierre et Marie Curie (Paris VI), France.

Dardenne, M.A., 2000. The Brasília fold belt. In: Cordani, U.G., Milani, E.J., Thomaz Filho, A., Campos, D.A. (Eds.), Tectonic Evolution of South America, Rio de Janeiro, Brazil, pp. 231–263.

Dardenne, M.A., Freitas-Silva, F.H., 1999. Pb–Zn ore deposits of Bambuí and Vazante Groups, in the São Francisco Craton and Brasília Fold Belt, Brazil. In: Silva, M.G., Misi, A. (Eds.), Base Metal Deposits of Brazil. MME/CPRM/DNPM, pp. 75–83.

Frimmel, H., Jonasson, I.R., Mubita, P., 2004. An Eburnean base metal source for sediment-hosted zinc–lead deposits in Neoproterozoic units of Namibia: lead isotope and geochemical evidence. Mineralium Deposita 39, 328–343.

Garven, G., Freeze, R.A., 1984. Theoretical analysis of the role of groundwater flow in the genesis of stratabound ore deposits 2: quantitative results. American Journal of Science 28, 1125–1174.

Golyshev, S.I., Padalko, N.L., Pechenkin, S.A., 1981. Fractionation of stable oxygen and carbon isotopes in carbonate systems. Geokhimiya 10, 1427–1441.

Grant, J.A., 1986. The isocon diagram — a simple solution to Gresens' equation for metasomatic alteration. Economic Geology 81, 1976–1982.

Gresens, R.L., 1967. Composition–volume relationships of metasomatism. Chemical Geology 2, 47–55.

Groves, I.M., Carman, C.E., Dunlap, W.J., 2003. Geology of the Beltana willemite deposit, Flinders Ranges, South Australia. Economic Geology 98, 797–818.

Hitzman, M.W., 1997. Sediment hosted Zn–Pb and Au deposits in the Proterozoic Paracatu–Vazante Fold Belt, Minas Gerais, Brazil. Geological Society of America Annual Meeting, Abstracts with Programs, vol. 29, p. A408.

Hitzman, M.W., Reynolds, N.A., Sangster, D.F., Allen, C.R., Carman, C.E., 2003. Classification, genesis, and exploration guides for nonsulfides zinc deposits. Economic Geology 98, 685–714.

Hoefs, J., 2004. Stable Isotope Geochemistry, Fifth edition. Springer, Berlin.

Iyer, S.S., Babinski, M., Krouse, H.R., Chemale Jr., F., 1995. Highly ^{13}C enriched carbonate and organic matter in the Neoproterozoic sediments of the Bambuí Group, Brazil. Precambrian Research 73, 271–282.

Kamona, A.F., Leveque, J., Friedrich, G., Haack, U., 1999. Lead isotopes of the carbonate-hosted Kabwe, Tsumeb, and Kipushi Pb–Zn–Cu sulphide deposits in relation to Pan-African orogenesis in the Damaran–Lufilian fold belt of Central Africa. Mineralium Deposita 34, 273–283.

Kampunzu, A.B., Wendorff, M., Kruge, F.J., Intiomale, M.M., 1998. Pb isotopic ages of sediment-hosted Pb–Zn mineralisation in the Neoproterozoic Copperbelt of Zambia and Democratic Republic of Congo (ex-Zaire), re-evaluation and implications. Chronique de la Recherche Minière 66, 55–61.

Kawashita, K., 1998. Rochas carbonáticas neoproterozóicas da América do Sul: idades e inferências quimioestratigráficas. Instituto de Geociências, Universidade de São Paulo.

Kucha, H., Wieczorek, A., 1984. Sulfide–carbonate relationships in the Navan (Tara) Zn–Pb Deposit Ireland. Mineralium Deposita 19, 208–216.

Le Huray, A.P., Caulfield, J.B.D., Rye, D.M., Dixon, P.R., 1987. Basements controls on sediment-hosted Zn–Pb deposits: a Pb isotope study of Carboniferous mineralization in Central Ireland. Economic Geology 82, 1695–1709.

Madalosso, A., Valle, C.R.O., 1978. Considerações sobre a estratigrafia e sedimentologia do Grupo Bambuí na Região de Paracatu–Morro Agudo (MG). 30th Congresso Brasileiro de Geologia, Recife, Anais, Sociedade Brasileira de Geologia, vol. 2, pp. 622–631.

McCrea, J.M., 1950. On the isotope chemistry of carbonates and palaeotemperature scale. Journal of Chemical Physics 18, 849–857.

Misi, A., 2001. Estratigrafia isotópica das seqüências do Supergrupo São Francisco, coberturas neoproterozóicas do Cráton do São Francisco. Idades e correlações. In: Pinto, C.P., Martins-Neto, M.A. (Eds.), Bacia do São Francisco: Geologia e Recursos Minerais. Sociedade Brasileira de Geologia / Minas Gerais, Belo Horizonte, pp. 67–92.

Misi, A., Iyer, S.S., Kyle, J.R., Coelho, C.E.S., Franca-Rocha, W.J.S., Gomes, A.S.R., Cunha, I.A., Carvalho, I.G., 1999. Geological and isotopic constraints on the metallogenic evolution of the Proterozoic sediment-hosted Pb–Zn (Ag) deposits of Brazil. Gondwana Research 2, 47–65.

Misi, A., Iyer, S.S.S., Coelho, C.E.S., Tassinari, C.C.G., Franca-Rocha, W.J.S., Cunha, I.A., Gomes, A.S.R., Oliveira, T.F., Teixeira, J.B.G., Filho, V.M.C., 2005. Sediment hosted lead–zinc deposits of the Neoproterozoic Bambuí Group and correlative sequences, São Francisco Craton, Brazil: a review and a possible metallogenetic evolution model. Ore Geology Reviews 26, 263–304.

Moeri, E., 1972. On a columnar stromatolite in the Precambrian Bambuí Group of Central Brazil. Eclogae Geologicae Helvetiae 65, 185–195.

Monteiro, L.V.S., 1997. Contribuição à gênese das mineralizações de zinco da Mina de Vazante, MG. Master thesis, Instituto Geociências, Universidade de São Paulo.

Monteiro, L.V.S., 2002. Modelamento metalogenético dos depósitos de zinco de Vazante, Fagundes e Ambrósia, associados ao Grupo Vazante, Minas Gerais. Ph.D. thesis, Universidade de São Paulo.

Monteiro, L.V.S., Bettencourt, J.S., Spiro, B., Graça, R., Oliveira, T.F., 1999. The Vazante zinc mine, MG, Brazil: constraints on fluid evolution and willemitic mineralization. Exploration and Mining Geology 8, 21–42.

Monteiro, L.V.S., Bettencourt, J.S., Oliveira, T.F., 2000. The Vazante, Ambrósia, and Fagundes (MG, Brazil) Neoproterozoic epigenetic zinc deposits: similarities, contrasting features, and genetic implications. 31st International Geological Congress, Rio de Janeiro, Brazil, Abstract volume. CD-ROM.

Monteiro, L.V.S., Bettencourt, J.S., Juliani, C., Oliveira, T.F., 2006. Geology, petrography, and mineral chemistry of the Vazante, Ambrósia, and Fagundes Neoproterozoic carbonate-hosted Zn–(Pb) deposits, Minas Gerais, Brazil. Ore Geology Reviews 28, 201–234.

Oliveira, T.F., 1998. As Minas de Vazante e de Morro Agudo. Workshop depósitos minerais brasileiros de metais base, Salvador, pp. 48–57. CPGG-UFBA/ADIMB.

Oliver, J., 1986. Fluids expelled tectonically from orogenic belts: their role in hydrocarbon migration and other geologic phenomena. Geology 14, 99–102.

Pimentel, M.M., Dardenne, M.A., Fuck, R.A., Viana, M.G., Junges, S.L., Fischel, D.P., Seer, H.J., Dantas, E.L., 2001. Nd isotopes and the provenance of detrital sediments of the Neoproterozoic Brasília Belt, Central Brazil. Journal of South American Earth Sciences 14, 571–585.

Pinho, J.M.M., 1990. Evolução tectônica da mineralização de zinco de Vazante. Master thesis, Instituto Geociências, Universidade de Brasília.

Pirajno, F., Joubert, B.D., 1993. An overview of carbonate-hosted mineral deposits in the Otavi Mountain Land, Namibia: implications for ore genesis. Journal of African Earth Sciences 16, 265–272.

Potdevin, J.L., 1993. Gresens 92: a simple Macintosh program of the Gresesn's method. Computers & Geosciences 19, 1229–1238.

Potdevin, J.L., Marquer, D., 1987. Méthodes de quantification des transferts de matière par les fluides dans les roches métamorphiques déformées. Geodinamica Acta 1, 193–206.

Rigobello, A.E., Branquinho, J.A., Dantas, M.G.S., Oliveira, T.F., Neves Filho, W., 1988. Mina de zinco de Vazante. In: Shobbenhaus, C., Coelho, C.E.S. (Coords.), Principais depósitos minerais do Brasil. Departamento Nacional Produção Mineral, Brazil, 3, 101–110.

Romagna, G., Costa, R.R., 1988. Jazida de zinco e chumbo de Morro Agudo, Paracatu, Minas Gerais. In: Shobbenhaus, C., Coelho, C.E.S. (coords). Principais Depósitos Minerais do Brasil. Departamento Nacional Produção Mineral, Brazil, 3, 111–121.

Savard, M.M., 1996. Pre-ore burial dolomitization adjacent to the carbonate-hosted Gays River Zn–Pb deposit, Nova Scotia. Canadian Journal of Earth Sciences 33, 303–315.

Veizer, J., 1983. Trace elements and isotopes in sedimentary carbonates. In: Reeder, R.J. (Ed.), Carbonates: Mineralogy and Chemistry Mineral. Reviews in Mineralogy, vol. 11, pp. 265–300.

Warren, J., 2000. Dolomite: occurrence, evolution and economically important associations. Earth-Science Reviews 52, 1–81.

Wilkinson, J.J., 2003. On diagenesis, dolomitisation and mineralization in the Irish Zn–Pb orefield. Mineralium Deposita 38, 968–983.

Zheng, Y.-F., Hoefs, J., 1993. Theoretical modeling on mixing processes and application to Pb–Zn deposits in the Harz Mountains, Germany. Mineralium Deposita 28, 79–89.